

Towards Yang-Baxter integrability of quantum crystal melting: From Kagome lattice to vertex models

Thiago Araujo

*Albert Einstein Center for Fundamental Physics,
Institute for Theoretical Physics, University of Bern
Sidlerstrasse 5, ch-3012, Bern, Switzerland*

`thiago@itp.unibe.ch`

Abstract

This paper considers aspects of a Kagome lattice system with states classified by plane partitions. Using two sets of free fermions, we rewrite the lattice as two families of spin chains. In this formalism, the quantum crystals Hamiltonian becomes more transparent, and we explicitly present the first 3 levels of plane partition states. A classical statistical model is also defined in terms of the Kagome lattice local configurations, and we show that it gives origin to two Yang-Baxter integrable subsystems related to a descendant of the 6-vertex model.

Contents

1	Introduction	2
2	Free fermions formulation	4
3	Classifying states with plane partitions	6
4	Kagome lattice Hamiltonian	10
5	Boltzmann weights & Classical Problem	11
6	Integrable (sub-) systems & Vertex models	19
7	Conclusions and Perspectives	25
	References	26

1 Introduction

Realistic exactly solvable models are incredibly rare, and that explains why the few examples we have are so celebrated. The Ising model, unarguably the best example, was once regarded as too simple, but nowadays, universality shows how it dictates the behavior of a vast collection of systems in science [1]. As a matter of fact, it is often believed that each university class has, at least, one integrable model where the critical exponents can be calculated.

From the mathematical perspective, it is known that exactly solvability generally means that there are conservation laws, symmetry groups, underlying the system dynamics. In this particular case, the wealth of mathematical structures might be less surprising, but these conservation laws generally imply a bidirectional interaction between physics and mathematics, see for example [2, 3].

In this work we study integrability properties of a statistical models of *plane partitions*. This is another pervasive system in theoretical physics, and has a rich and long tradition in mathematics [4]. Statistical models of plane partitions emerge from supersymmetric gauge theories, black holes and in the AdS/Higher Spins correspondence [5–9]; and inspired by these developments, we aim to study quantum aspects of this system.

More specifically, we study the *quantum crystal melting* problem. It is a dynamical system akin to the combinatorics of plane partitions, and that can be rephrased in terms of dimers in an hexagonal lattice 1a. Although the exactly solvability of this problem and its relation to physical problems become more evident in the later description [8, 10], the understanding of how the Yang-Baxter equation, a hallmark for integrability, emerge in the quantum crystal melting problem is still lacking.



(a) 1-Box configuration in terms of dimers. (b) Empty partition in the Kagome lattice.

Figure 1: Partitions as Dimers and in the Kagome lattice.

A quantum crystal melting Hamiltonian has been found by the authors [11], and among their findings, the following observations are particularly noteworthy. The 1D and 2D Hamiltonians are exactly solvable; in fact, the authors have shown that 2D system is the XXZ model in disguise. This fact naturally implies the Bethe solvability of the 2D quantum crystal melting Hamiltonian [12]. Additionally, the 1D and 2D have the same mass gap. These results (and further numerical analysis) led the authors to conjecture that the 3D version of the quantum crystal melting problem is also integrable, and has the mass gap of its lower dimensional cousins.

The Hamiltonian in [11] is written as

$$H = -J \sum |\blacksquare\rangle\langle\Box| + |\Box\rangle\langle\blacksquare| + V \sum \sqrt{q}|\Box\rangle\langle\Box| + \frac{1}{\sqrt{q}}|\blacksquare\rangle\langle\blacksquare|, \quad (1.1)$$

where the first two terms describe the creation and annihilation of boxes in a given plane partition configuration; and the diagonal terms define an asymmetric diffusion process, where $|\Box\rangle\langle\Box|$ gives

the number of places where we can consistently add a box, and $|\blacksquare\rangle\langle\blacksquare|$ gives the number of boxes that can be removed from a given configuration.

We have addressed several questions of the 3D Hamiltonian in [13], in particular a novel fermion-boson correspondence for plane partitions, which generalizes the usual two dimensional duality, has been found. We have also shown that the bosonized partition states are closely related to the MacMahon representation of the affine Yangian $\mathcal{Y}[\hat{\mathfrak{gl}}(1)]$ as defined by [9, 14, 15]. One realization of Yangians is given in terms of the RTT-relation, where T denotes the monodromy matrix and R a solution of the Yang-Baxter equation [16]. Although the presence of the $\mathcal{Y}[\hat{\mathfrak{gl}}(1)]$ algebra denotes an underlying integrable structure in this problem, a more pragmatcal relation between the Yangian algebra above and the quantum crystal melting still eludes us.

Using the well known equivalence between plane partitions and dimers in an hexagonal lattice, see figure 1b, we have also shown how the quantum crystal growth can be translated into an occupation problem in a Kagome lattice, and this is the viewpoint we want to push forward in the current work.

In section 2 we consider a rotation of $-\pi/6$ in the Kagome lattice system [13], and we rewrite it using two independent families of free fermions defined by their generating functions $\psi^{(a)}(z)$ and $\theta^{(a)}(z)$. With this definition, we show that the lattice model is equivalent to two sets of spin chains that we call the $X^{(a)}$ and $Y^{(b)}$ -type spin chains. The vacuum configuration is represented graphically in 2a, where the big white circle denotes the plaquette where the flip (box creation) can be performed.

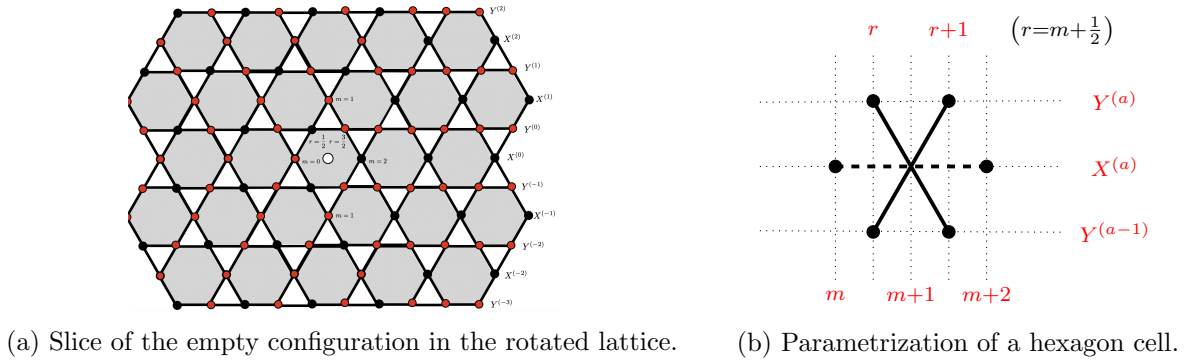


Figure 2: Empty partition and hexagon cell parametrization.

In section 3, using the parametrization of figure 2b, we rewrite the quantum Hamiltonian (1.1) as a series of coupled spin chains. We show that after a Jordan-Wigner transformation the system can be written in terms of two families of $su(2)$ generators – it should be contrasted with the 2D case of [11]. In the analysis of section 4, the growth operators for the crystal melting Hamiltonian are represented in terms of this new parametrization, and we also find explicit expressions for the Kagome lattice states corresponding to the 0-, 1- and 2-boxes plane partition configurations.

Section 5 describes the allowed local hexagon configurations in the lattice, and we also assign a Boltzmann weight to each local configuration. As an interesting consequence, we associate a classical statistical system to the crystal melting defined in terms of the Kagome lattice. In section 6, we use the transfer matrix method to study this associated classical system, and we also show that it can be built from a descendant of the 6-vertex model. In section 7 we conclude with a short discussion and an overview on future research directions.

2 Free fermions formulation

Now we define a new parametrization for the study of plane partition growth in the Kagome lattice. A throughout description of the relation between plane partitions and its Kagome lattice formulation can be found in [13].

2.1 X-type spin chains

In order to define the $X^{(a)}$ -type spin chains, let us start with some well known facts [2, 3, 11]. The components of the free fermions $\psi^{(a)}(z) = \sum_m \psi_m^{(a)} z^m$, with $a \in \mathbb{Z}$, satisfy the canonical anticommutation relations

$$\{\psi_m^{(a)}, \psi_n^{*(b)}\} = \delta^{ab} \delta_{mn} \quad \{\psi_m^{(a)}, \psi_n^{(b)}\} = \{\psi_m^{*(a)}, \psi_n^{*(b)}\} = 0 \quad \forall m, n, a, b \in \mathbb{Z}. \quad (2.1)$$

The operators $\eta_m^{(a)} = \psi_m^{(a)} \psi_m^{*(a)}$ and $\bar{\eta}_m^{(a)} = \psi_m^{*(a)} \psi_m^{(a)}$ count, respectively, the number of holes and particles in a given site in the chain. The *vacuum* $|0\rangle$ is the state satisfying

$$\psi_n^{(a)}|0\rangle = 0, \quad n \leq 0, \quad \psi_n^{*(a)}|0\rangle = 0, \quad n > 0, \quad \forall a \in \mathbb{Z}. \quad (2.2)$$

This corresponds to a configuration where all positive (-labeled) sites, $n > 0$, are occupied by particles, see figure 3. Additionally, the shifted vacuum is defined by the relations

$$|m\rangle^{(a)} = \begin{cases} \psi_m^{(a)} \cdots \psi_2^{(a)} \psi_1^{(a)} |0\rangle & m > 0 \\ \psi_{m+1}^{*(a)} \cdots \psi_{-1}^{*(a)} \psi_0^{*(a)} |0\rangle & m < 0 \end{cases}. \quad (2.3)$$

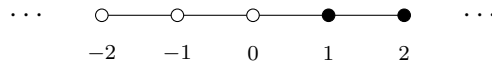


Figure 3: Vacuum.

The $X^{(a)}$ -spin chains are defined by the relations above, and two additional properties that we describe now. There is a *zigzag* between the even (-labeled) rows $X^{(2a)}$ and the odd (-labeled) rows $X^{(2a+1)}$. More specifically, if particles in the even rows are localized at the positions $m d_X$, where $m \in \mathbb{Z}$ and d_X is the lattice distance, the odd chains particles are positioned at $(m + 1/2) d_X$. Additionally, inspection of figure 2a shows that the lattice distance d_X in the X-rows is twice the Y-chains lattice distance d_Y that, without any loss of generality, we normalize as $d_Y = 1$.

In order to address these two points at once, we parametrize even (odd) rows with even (odd) indices. Moreover, when we assumed $d_Y = 1$, we have automatically rescaled the lattice distance in the lines $X^{(a)}$ by a factor of two. Consequently, if $[0], [1] \in \mathbb{Z}/2\mathbb{Z}$ are the equivalence classes of even and odd integers, respectively, we define the vacuum in the even X rows, the *even vacuum* $|\mathbf{0}\rangle$, as

$$\psi_n^{(a)}|\mathbf{0}\rangle^{(a)} = 0 \quad n \in [0] \leq 0, \quad \psi_n^{*(a)}|\mathbf{0}\rangle^{(a)} = 0 \quad n \in [0] > 0, \quad \forall a \in [0] \quad (2.4)$$

represented as 4a; and the vacuum $|\mathbf{1}\rangle$ in the odd X rows, the *odd vacuum* as

$$\begin{aligned} \psi_n^{(a)}|\mathbf{1}\rangle^{(a)} &= 0 \quad n \in [1] \leq 0, \\ \psi_n^{*(a)}|\mathbf{1}\rangle^{(a)} &= 0 \quad n \in [1] > 0 \end{aligned}, \quad \forall a \in [1] \quad (2.5)$$



Figure 4: Even and odd vacua.

represented as 4b.

Finally, the shifted even and odd vacua are respectively

$$|\mathbf{m}\rangle^{(a)} = \begin{cases} \psi_m^{(a)} \cdots \psi_4^{(a)} \psi_2^{(a)} |\mathbf{0}\rangle & m \in [0] > 0 \\ \psi_{m+2}^{*(a)} \cdots \psi_{-2}^{*(a)} \psi_0^{*(a)} |\mathbf{0}\rangle & m \in [0] < 0 \end{cases}, \quad \forall a \in [0] \quad (2.6a)$$

and

$$|\mathbf{m}\rangle^{(a)} = \begin{cases} \psi_m^{(a)} \cdots \psi_5^{(a)} \psi_3^{(a)} |\mathbf{1}\rangle & m \in [1] > 1 \\ \psi_{m+2}^{*(a)} \cdots \psi_{-1}^{*(a)} \psi_1^{*(a)} |\mathbf{1}\rangle & m \in [1] < 1 \end{cases}, \quad \forall a \in [1]. \quad (2.6b)$$

As we see in a later section, the definitions above fully characterize the X -spin chains in the Kagome lattice. Before addressing this point, let us now move to the Y -spin chains.

2.2 Y-type spin chains

This case is more straightforward, and we simply consider fermionic operators defined by their anticommutation relations

$$\{\theta_r^{(a)}, \theta_s^{*(b)}\} = \delta^{ab} \delta_{rs} \quad \{\theta_r^{(a)}, \theta_s^{(b)}\} = \{\theta_r^{(a)}, \theta_s^{(b)}\} = 0 \quad \forall r, s \in \mathbb{Z} + \frac{1}{2}. \quad (2.7)$$

The differences with relation to the X -rows start with the number operators $\zeta_r^{(a)} = \theta_r^{*(a)} \theta_r^{(a)}$ and $\bar{\zeta}_r^{(a)} = \theta_r^{(a)} \theta_r^{*(a)}$. These operators count, respectively, the number of particles and holes in the $Y^{(a)}$ chain. Observe that their structures are different from the number operators η and $\bar{\eta}$. These definitions have been used in [11] to rewrite the integer partition problem in terms of the XXZ-Hamiltonian with kink boundary conditions.

Fortunately, there is no zigzag between even and odd Y -rows as in the X -rows case, and we do not need to modify the conventions above. The vacuum $|\tilde{\mathbf{0}}\rangle$ is given by

$$\theta_r^{(a)} |\tilde{\mathbf{0}}\rangle^{(a)} = 0, \quad r > 0, \quad \theta_r^{*(a)} |\tilde{\mathbf{0}}\rangle^{(a)} = 0, \quad r < 0, \quad \forall a \in \mathbb{Z}, \quad (2.8)$$

and it corresponds to the configuration in figure 5, where all negative half-integers ($r < 0$) positions are occupied by particles.

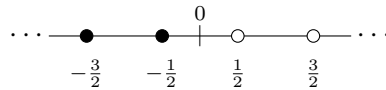


Figure 5: Vacuum in the Y -rows.

Finally, the shifted vacua of the Y -rows are

$$|\tilde{\ell}\rangle^{(a)} = \begin{cases} \theta_{\ell+1/2}^{(a)} \cdots \theta_{-3/2}^{(a)} \theta_{-1/2}^{(a)} |\tilde{\mathbf{0}}\rangle & \ell < 0 \\ \theta_{\ell-1/2}^{*(a)} \theta_{\ell-3/2}^{*(a)} \cdots \theta_{1/2}^{*(a)} |\tilde{\mathbf{0}}\rangle & \ell > 0 \end{cases} \quad \ell \in \mathbb{Z}. \quad (2.9)$$

3 Classifying states with plane partitions

Now we want to use the definitions above to write the states classified by plane partitions. We first define the empty partition state, that is the subtler state in the Hilbert space. Explicit expressions for states with more boxes are laborious, but are trivial from the formal perspective.

0-box

Let us start with the empty partition $|\emptyset\rangle$. Using figure 2a, it is easy to see that the X-rows contribute as

$$\begin{aligned} |\emptyset_X\rangle &= \bigotimes_{a \in \mathbb{Z}} |a\rangle^{(a)} \\ &= \dots \otimes |\mathbf{2}\rangle^{(-2)} \otimes |\mathbf{1}\rangle^{(-1)} \otimes |\mathbf{0}\rangle^{(0)} \otimes |\mathbf{1}\rangle^{(1)} \otimes |\mathbf{2}\rangle^{(2)} \otimes \dots \end{aligned} \quad (3.1)$$

The Y-rows are more involved. We start with the definition of two fiducial states, namely

$$|y_1\rangle^{(a)} := \prod_{i \in \mathbb{Z}^{\geq 0}} \theta_{-(4i+1)/2} |\tilde{\mathbf{0}}\rangle, \quad (3.2)$$

that corresponds to the configuration in figure 6a and

$$|y_2\rangle^{(a)} := \prod_{i \in \mathbb{Z}^{\geq 0}} \theta_{-(4i+3)/2} |\tilde{\mathbf{0}}\rangle, \quad (3.3)$$

that corresponds to the configuration in figure 6b.

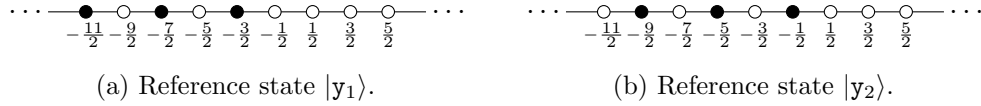


Figure 6: Fiducial states $|y_1\rangle$ and $|y_2\rangle$.

We also need to define the states

$$|(4\ell + 1)/2\rangle^{(a)} = \prod_{i=0}^{\ell} \theta_{(4i+1)/2} |y_1\rangle^{(a)} \quad (3.4a)$$

and

$$|(4\ell + 3)/2\rangle^{(a)} = \prod_{i=0}^{\ell} \theta_{(4i+3)/2} |y_2\rangle^{(a)}, \quad (3.4b)$$

for $\ell \in \mathbb{Z}^{\geq 0}$. The Y-rows contribute to the empty configuration state as

$$\begin{aligned} |\emptyset_Y\rangle &= \bigotimes_{a \in \mathbb{Z}^{\geq 0}} \left(|(2a + 1)/2\rangle^{(a)} \otimes |(2a + 1)/2\rangle^{(-a-1)} \right) \\ &= |\mathbf{1}/2\rangle^{(0)} \otimes |\mathbf{1}/2\rangle^{(-1)} \otimes |\mathbf{3}/2\rangle^{(1)} \otimes |\mathbf{3}/2\rangle^{(-2)} \otimes \dots \end{aligned} \quad (3.5)$$

All in all, the empty configuration is written as

0-box configuration

$$|\emptyset\rangle = |\emptyset_X\rangle \otimes |\emptyset_Y\rangle . \quad (3.6)$$

Before studying states with more boxes, let us define the number operator

$$\sum |\square\rangle\langle\square| = \sum_{\substack{a \in \mathbb{Z}; m \in [a] \\ r \in \mathbb{Z} + \frac{1}{2}}} \zeta_r^{(a)} \bar{\zeta}_{r+1}^{(a)} \zeta_r^{(a-1)} \bar{\zeta}_{r+1}^{(a-1)} \eta_m^{(a)} \bar{\eta}_{m+2}^{(a)} \quad (3.7a)$$

that counts the number of available places in a given configuration, and

$$\sum |\blacksquare\rangle\langle\blacksquare| = \sum_{\substack{a \in \mathbb{Z}; m \in [a] \\ r \in \mathbb{Z} + \frac{1}{2}}} \zeta_{r+1}^{(a)} \bar{\zeta}_r^{(a)} \zeta_{r+1}^{(a-1)} \bar{\zeta}_r^{(a-1)} \eta_{m+2}^{(a)} \bar{\eta}_m^{(a)} \quad (3.7b)$$

that gives the number of boxes that can be consistently removed from the corresponding plane partition.

Their action on the empty partition state give

$$\sum |\square\rangle\langle\square|\emptyset\rangle = \zeta_{1/2}^{(0)} \bar{\zeta}_{3/2}^{(0)} \zeta_{1/2}^{(-1)} \bar{\zeta}_{3/2}^{(-1)} \eta_0^{(0)} \bar{\eta}_2^{(0)} |\emptyset\rangle = |\emptyset\rangle , \quad (3.8a)$$

and

$$\sum |\blacksquare\rangle\langle\blacksquare|\emptyset\rangle = \zeta_{3/2}^{(0)} \bar{\zeta}_{1/2}^{(0)} \zeta_{3/2}^{(-1)} \bar{\zeta}_{1/2}^{(-1)} \eta_2^{(0)} \bar{\eta}_0^{(0)} |\emptyset\rangle = 0 . \quad (3.8b)$$

It naturally means that in the 0-box state we do not have any box to be removed and there is one available place to add a box. Finally, the box-annihilation and -creation operators are defined as follows

$$\sum |\square\rangle\langle\blacksquare| = \sum_{\substack{a \in \mathbb{Z}; m \in [a] \\ r \in \mathbb{Z} + \frac{1}{2}}} \theta_r^{*(a)} \theta_{r+1}^{(a)} \theta_r^{*(a-1)} \theta_{r+1}^{(a-1)} \psi_{m+2}^{*(a)} \psi_m^{(a)} \quad (3.9a)$$

and

$$\sum |\blacksquare\rangle\langle\square| = \sum_{\substack{a \in \mathbb{Z}; m \in [a] \\ r \in \mathbb{Z} + \frac{1}{2}}} \theta_{r+1}^{*(a)} \theta_r^{(a)} \theta_{r+1}^{*(a-1)} \theta_r^{(a-1)} \psi_m^{*(a)} \psi_{m+2}^{(a)} . \quad (3.9b)$$

Let us now act with $\sum |\square\rangle\langle\blacksquare|$ and $\sum |\blacksquare\rangle\langle\square|$ on $|\emptyset\rangle$. Initially we have

$$\sum |\square\rangle\langle\blacksquare|\emptyset\rangle = 0 , \quad (3.10)$$

that logically annihilates the empty configuration. In other words, it is the highest weight state in this representation, and states with more boxes are obtained from the action of the box-creation operator.

1-box

From the considerations above, the 1-box configuration is

1-box configuration

$$\begin{aligned} |\square\rangle &\equiv \sum |\blacksquare\rangle \langle \square | \emptyset \rangle \\ &= \theta_{3/2}^{*(0)} \theta_{1/2}^{(0)} \theta_{3/2}^{*(-1)} \theta_{1/2}^{(-1)} \psi_0^{*(0)} \psi_2^{(0)} |\emptyset\rangle \end{aligned} \quad (3.11)$$

We say that it is the 1-box plane partition state with lattice configuration given by figure 7. The big white circle in 2a denotes the plaquette where the particles hopping (box creation) can be performed, and the big yellow circle denotes the plaquette where the box-annihilation operator acts in a nontrivial manner.

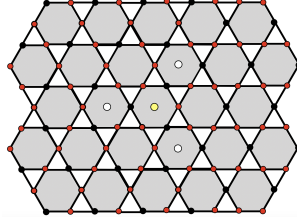


Figure 7: Lattice configuration $|\square\rangle$.

The number operators now give

$$\left(\sum |\blacksquare\rangle \langle \blacksquare| \right) |\square\rangle = \zeta_{3/2}^{(0)} \bar{\zeta}_{1/2}^{(0)} \zeta_{3/2}^{(-1)} \bar{\zeta}_{1/2}^{(-1)} \eta_2^{(0)} \bar{\eta}_0^{(0)} |\square\rangle = |\square\rangle, \quad (3.12a)$$

which says that we have one box to remove from this configuration. Furthermore, the condition

$$\begin{aligned} \left(\sum |\square\rangle \langle \square| \right) |\square\rangle &= \zeta_{3/2}^{(-1)} \bar{\zeta}_{5/2}^{(-1)} \zeta_{3/2}^{(-2)} \bar{\zeta}_{5/2}^{(-2)} \eta_1^{(-1)} \bar{\eta}_3^{(-1)} |\square\rangle \\ &\quad + \zeta_{-3/2}^{(0)} \bar{\zeta}_{-1/2}^{(0)} \zeta_{-3/2}^{(-1)} \bar{\zeta}_{-1/2}^{(-1)} \eta_{-2}^{(0)} \bar{\eta}_0^{(0)} |\square\rangle \\ &\quad + \zeta_{3/2}^{(1)} \bar{\zeta}_{5/2}^{(1)} \zeta_{3/2}^{(0)} \bar{\zeta}_{5/2}^{(0)} \eta_1^{(1)} \bar{\eta}_3^{(1)} |\square\rangle \\ &= 3 |\square\rangle. \end{aligned} \quad (3.12b)$$

means that we have three available places to add a second box.

We now apply the growth operators to the lattice state corresponding to the 1-box state. First, it is easy to see that

$$\left(\sum |\square\rangle \langle \blacksquare| \right) |\square\rangle = |\emptyset\rangle, \quad (3.13)$$

since there is one box to be removed consistently.

2-boxes

Finally, acting with the creation operator we have

$$\begin{aligned}
\left(\sum |\blacksquare\rangle \langle \square| \right) |\square\rangle &= \sum_{m \in [1]} \theta_{m+3/2}^{*(-1)} \theta_{m+1/2}^{(-1)} \theta_{m+3/2}^{*(-2)} \theta_{m+1/2}^{(-2)} \psi_m^{*(-1)} \psi_{m+2}^{(-1)} |\square\rangle + \\
&+ \sum_{m \in [1]} \theta_{m+3/2}^{*(1)} \theta_{m+1/2}^{(1)} \theta_{m+3/2}^{*(0)} \theta_{m+1/2}^{(0)} \psi_m^{*(1)} \psi_{m+2}^{(1)} |\square\rangle \\
&+ \sum_{m \in [0]} \theta_{m+3/2}^{*(0)} \theta_{m+1/2}^{(0)} \theta_{m+3/2}^{*(-1)} \theta_{m+1/2}^{(-1)} \psi_m^{*(0)} \psi_{m+2}^{(0)} |\square\rangle
\end{aligned} \tag{3.14a}$$

where we represent these states in terms of 2-boxes partitions as

2-boxes configurations

$$|\square\square\rangle = \theta_{5/2}^{*(-1)} \theta_{3/2}^{(-1)} \theta_{5/2}^{*(-2)} \theta_{3/2}^{(-2)} \psi_1^{*(-1)} \psi_3^{(-1)} |\square\rangle \tag{3.14b}$$

$$|\square\rangle = \theta_{5/2}^{*(1)} \theta_{3/2}^{(1)} \theta_{5/2}^{*(0)} \theta_{3/2}^{(0)} \psi_1^{*(1)} \psi_3^{(1)} |\square\rangle \tag{3.14c}$$

$$|\square 2\rangle = \theta_{-1/2}^{*(0)} \theta_{-3/2}^{(0)} \theta_{-1/2}^{*(-1)} \theta_{-3/2}^{(-1)} \psi_{-2}^{*(1)} \psi_0^{(1)} |\square\rangle \tag{3.14d}$$

These states are written diagrammatically in figures 8a, 8b and 8c, respectively. We also represent the locked plane partition box with a big blue circle.

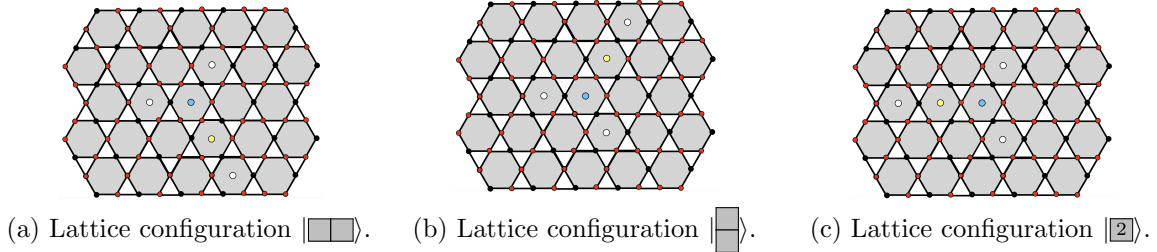


Figure 8: States corresponding to 2-boxes plane partitions.

Evidently we can build states with more boxes in a similar way, but now we want to study other aspects of this model. Diagonalization of the Hamiltonian (4.1a) is a problem we could not address in this work, but from [11], we know that its ground state is

$$|\Psi_0\rangle = \sum_{\Lambda} q^{\frac{\#Boxes(\Lambda)}{2}} |\Lambda\rangle, \tag{3.15}$$

in such a way that its norm squared gives that famous MacMahon function

$$\langle \Psi_0 | \Psi_0 \rangle = \prod_n \frac{1}{(1 - q^n)^n}. \tag{3.16}$$

4 Kagome lattice Hamiltonian

As we said before, in [13] we have rewritten the Hamiltonian (1.1) in terms of fermions in a Kagome lattice. Furthermore, the plane partition classification of states is a level grading; and for each plane partition configuration, there is a corresponding state in the Kagome lattice. In this section, we want to continue this analysis using the parametrization of section (2).

Remember that the box creation and annihilation are equivalent to simultaneous particles hopping in the Kagome lattice hexagon. In the X and Y -spin chains parametrization, such hexagons live in the triads $Y^{(a)}-X^{(a)}-Y^{(a-1)}$, and box creation and annihilation are represented as in figures 9a and 9b.

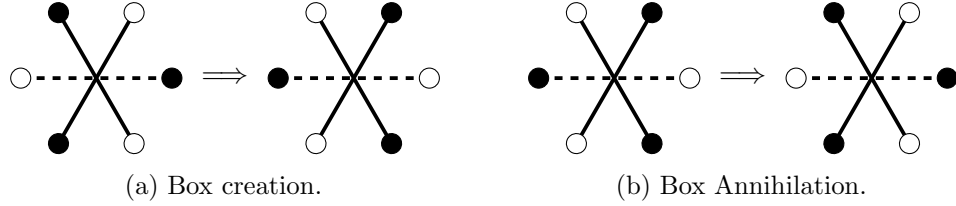


Figure 9: Box creation and annihilation from the hexagon cell perspective.

Using these simple observations, the parametrization defined in section (2) and the operators (3.7a), (3.7b), (3.9a) and (3.9b), it is easy to convince ourselves that the Hamiltonian (1.1) is equivalent to

$$\begin{aligned}
 H = -J \sum_{\substack{a \in \mathbb{Z}; m \in [a] \\ r=m+\frac{1}{2}}} & \left[\theta_r^{*(a)} \theta_{r+1}^{(a)} \theta_r^{*(a-1)} \theta_{r+1}^{(a-1)} \psi_{m+2}^{*(a)} \psi_m^{(a)} + \theta_{r+1}^{*(a)} \theta_r^{(a)} \theta_{r+1}^{*(a-1)} \theta_r^{(a-1)} \psi_m^{*(a)} \psi_{m+2}^{(a)} \right. \\
 & \left. - \frac{V\sqrt{q}}{J} \zeta_r^{(a)} \bar{\zeta}_{r+1}^{(a)} \zeta_r^{(a-1)} \bar{\zeta}_{r+1}^{(a-1)} \eta_m^{(a)} \bar{\eta}_{m+2}^{(a)} - \frac{V}{J\sqrt{q}} \zeta_{r+1}^{(a)} \bar{\zeta}_r^{(a)} \zeta_{r+1}^{(a-1)} \bar{\zeta}_r^{(a-1)} \eta_{m+2}^{(a)} \bar{\eta}_m^{(a)} \right], \quad (4.1a)
 \end{aligned}$$

where $[a]$ denotes the equivalence classes of $\mathbb{Z}/2\mathbb{Z}$, which is a manifestation of the X -rows zigzag between even and odd rows. It is easy to see that the Hamiltonian has two parts: one of them acts on the triad $Y^{(2a)}-X^{(2a)}-Y^{(2a-1)}$, and another on $Y^{(2a+1)}-X^{(2a+1)}-Y^{(2a)}$, therefore

$$\boxed{H = \sum_{\substack{a,m \\ (r=2m+1/2)}} H_{2a,2m} + \sum_{\substack{a,m \\ (r=2m+3/2)}} H_{2a+1,2m+1}} \quad (4.1b)$$

or more explicitly

$$\begin{aligned}
 H = -J \sum_{\substack{a \in \mathbb{Z}; m \in [a] \\ r=m+\frac{1}{2}}} & \left[\left(\theta_r^{*(2a)} \theta_{r+1}^{(2a)} \theta_r^{*(2a-1)} \theta_{r+1}^{(2a-1)} \psi_{2m+2}^{*(2a)} \psi_{2m}^{(2a)} + \theta_{r+1}^{*(2a)} \theta_r^{(2a)} \theta_{r+1}^{*(2a-1)} \theta_r^{(2a-1)} \psi_{2m}^{*(2a)} \psi_{2m+2}^{(2a)} \right. \right. \\
 & + \theta_r^{*(2a+1)} \theta_{r+1}^{(2a+1)} \theta_r^{*(2a)} \theta_{r+1}^{(2a)} \psi_{2m+3}^{*(2a+1)} \psi_{2m+1}^{(2a+1)} + \theta_{r+1}^{*(2a+1)} \theta_r^{(2a+1)} \theta_{r+1}^{*(2a)} \theta_r^{(2a)} \psi_{2m+1}^{*(2a+1)} \psi_{2m+3}^{(2a+1)} \Big) \\
 & - \frac{V\sqrt{q}}{J} \left(\zeta_r^{(2a)} \bar{\zeta}_{r+1}^{(2a)} \zeta_r^{(2a-1)} \bar{\zeta}_{r+1}^{(2a-1)} \eta_{2m}^{(2a)} \bar{\eta}_{2m+2}^{(2a)} + \zeta_r^{(2a+1)} \bar{\zeta}_{r+1}^{(2a+1)} \zeta_r^{(2a)} \bar{\zeta}_{r+1}^{(2a)} \eta_{2m+1}^{(2a+1)} \bar{\eta}_{2m+3}^{(2a+1)} \right) \\
 & \left. - \frac{V}{J\sqrt{q}} \left(\zeta_{r+1}^{(2a)} \bar{\zeta}_r^{(2a)} \zeta_{r+1}^{(2a-1)} \bar{\zeta}_r^{(2a-1)} \eta_{2m+2}^{(2a)} \bar{\eta}_{2m}^{(2a)} + \zeta_{r+1}^{(2a+1)} \bar{\zeta}_r^{(2a+1)} \zeta_{r+1}^{(2a)} \bar{\zeta}_r^{(2a)} \eta_{2m+3}^{(2a+1)} \bar{\eta}_{2m+1}^{(2a+1)} \right) \right]. \quad (4.1c)
 \end{aligned}$$

As we mentioned before, the 2D version of (1.1) has been mapped to the XXZ-Hamiltonian in [11] using a Jordan-Wigner transformation. With the parametrization that we have defined in section (2), we can apply the same idea to the 3D problem but, as we see below, the final result is not so appealing. Let us first denote the states in a given site as $|\bullet\rangle \equiv |+\rangle \equiv |\uparrow\rangle$ and $|\circ\rangle \equiv |-\rangle \equiv |\downarrow\rangle$. The Jordan-Wigner transformation gives the following map between free fermions and the fundamental representation of the $su(2)$ algebra

$$\begin{aligned} \psi_m^{*(a)}|\bullet\rangle_m = 0 & \Leftrightarrow \begin{aligned} \chi_m^{+(a)}|+\rangle_m &= 0 \\ \chi_m^{-(a)}|-\rangle_m &= 0 \\ \chi_m^{z(a)}|\pm\rangle_m &= \pm\frac{1}{2}|\pm\rangle_m \end{aligned} & \theta_r^{*(a)}|\bullet\rangle_r = 0 & \Leftrightarrow \begin{aligned} \tau_r^{+(a)}|+\rangle_r &= 0 \\ \tau_r^{-(a)}|-\rangle_r &= 0 \\ \tau_r^{z(a)}|\pm\rangle_r &= \pm\frac{1}{2}|\pm\rangle_r \end{aligned} \end{aligned} \quad (4.2)$$

where $\vec{\chi}$ and $\vec{\xi}$ satisfy the $su(2)$ algebra

$$\begin{aligned} [\chi_+, \chi_-] &= 2\chi^z & [\chi_z, \chi_\pm] &= \pm\chi^\pm \\ [\xi_+, \xi_-] &= 2\xi^z & [\xi_z, \xi_\pm] &= \pm\xi^\pm \end{aligned} \quad (4.3)$$

The number operators act in a very straightforward manner

$$\begin{aligned} \eta_m|\bullet\rangle_m = 0 & \quad \eta_m|\circ\rangle_m = |\circ\rangle_m & \zeta_r|\bullet\rangle_r = |\bullet\rangle_r & \quad \zeta_r|\circ\rangle_r = 0 \\ \bar{\eta}_m|\bullet\rangle_m = |\bullet\rangle_m & \quad \bar{\eta}_m|\circ\rangle_m = 0 & \bar{\zeta}_r|\bullet\rangle_r = 0 & \quad \bar{\zeta}_r|\circ\rangle_r = |\circ\rangle_r \end{aligned} \quad (4.4)$$

In terms of the $su(2)$ generators, the Hamiltonian (4.1a) can be inelegantly expressed as

$$\begin{aligned} H = -J \sum_{\substack{a \in \mathbb{Z}; m \in [a] \\ r \in \mathbb{Z} + \frac{1}{2}}} & \left\{ \tau_r^{+(a)} \tau_{r+1}^{-(a)} \tau_r^{+(a-1)} \tau_{r+1}^{-(a-1)} \chi_{m+2}^{+(a)} \chi_m^{-(a)} + \tau_{r+1}^{+(a)} \tau_r^{-(a)} \tau_{r+1}^{+(a-1)} \tau_r^{-(a-1)} \chi_m^{+(a)} \chi_{m+2}^{-(a)} \right. \\ & - \frac{V\sqrt{q}}{J} \left[\frac{1}{2} \left(\tau_r^{z(a)} - \tau_{r+1}^{z(a)} \right) - \tau_r^{z(a)} \tau_{r+1}^{z(a)} + \frac{1}{4} \right] \left[\frac{1}{2} \left(\tau_r^{z(a-1)} - \tau_{r+1}^{z(a-1)} \right) - \tau_r^{z(a-1)} \tau_{r+1}^{z(a-1)} + \frac{1}{4} \right] \times \\ & \quad \left[\frac{1}{2} \left(\chi_{m+2}^{z(a)} - \chi_m^{z(a)} \right) - \chi_m^{z(a)} \chi_{m+2}^{z(a)} + \frac{1}{4} \right] \\ & - \frac{V}{J\sqrt{q}} \left[\frac{1}{2} \left(\tau_{r+1}^{z(a)} - \tau_r^{z(a)} \right) - \tau_{r+1}^{z(a)} \tau_r^{z(a)} + \frac{1}{4} \right] \left[\frac{1}{2} \left(\tau_{r+1}^{z(a-1)} - \tau_r^{z(a-1)} \right) - \tau_{r+1}^{z(a-1)} \tau_r^{z(a-1)} + \frac{1}{4} \right] \times \\ & \quad \left. \left[\frac{1}{2} \left(\chi_m^{z(a)} - \chi_{m+2}^{z(a)} \right) - \chi_{m+2}^{z(a)} \chi_m^{z(a)} + \frac{1}{4} \right] \right\}, \end{aligned} \quad (4.5)$$

and we see that contrary to the 2D case, the resulting plane partition Hamiltonian in terms of $su(2)$ generators does not make the problem any easier.

5 Boltzmann weights & Classical Problem

As we have seen in section (4), the Kagome lattice Hamiltonian can be decomposed in terms of even and odd parts as

$$\begin{aligned} H &= \sum_{\substack{a, m \in \mathbb{Z} \\ r \in \mathbb{Z} + \frac{1}{2}}} \mathcal{H}_{a, m} = \sum_{\substack{a, m \in \mathbb{Z} \\ r \in \mathbb{Z} + \frac{1}{2}}} (H_{2a, 2m} + H_{2a+1, 2m+1}) \\ &\equiv H_{(even)} + H_{(odd)}. \end{aligned} \quad (5.1)$$

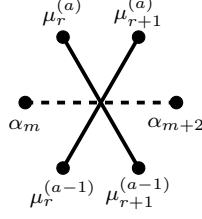


Figure 10: Hexagon.

We consider now that the system lives in a finite lattice, say with N triads YXY -rows and M columns (or hexagons) in each YXY -triad. Moreover, periodic boundary conditions are imposed in both directions; in other words, the system lives in a torus $\mathbb{Z}_M \times \mathbb{Z}_N$. The partition function is given by

$$\begin{aligned} Z &= \text{Tr} \left(e^{-\beta H} \right) \\ &= \text{Tr} \left[\exp \left(-\beta \sum_{a,m \in \mathbb{Z}} (H_{2a,2m} + H_{2a+1,2m+1}) \right) \right], \end{aligned} \quad (5.2a)$$

where $\beta \equiv 1/\kappa_B T$. Since $[\mathcal{H}_{a,m}, \mathcal{H}_{a,m\pm 1}] \neq 0$, $[\mathcal{H}_{a,m}, \mathcal{H}_{a\pm 1,m}] \neq 0$ and $[\mathcal{H}_{a,m}, \mathcal{H}_{a\pm 1,m\pm 1}] \neq 0$, we cannot split the partition function in terms of products of local operators. Using the Zassenhaus formula – the dual Baker-Campbell-Hausdorff formula – the partition function can be written as

$$Z = \text{Tr} \left(e^{-\beta H_{(even)}} e^{-\beta H_{(odd)}} \prod_{n \geq 2} e^{C_n(H_{(even)}, H_{(odd)})} \right), \quad (5.2b)$$

where $C_n(H_{(even)}, H_{(odd)})$ are homogeneous polynomials in $H_{(even)}$ and $H_{(odd)}$ of degree n .

As usual, in order to compute this partition function we need to diagonalize the Hamiltonian H to determine the eigenvalues $E_{\mathcal{C}}$ of the eigenstates $|\Psi(\mathcal{C})\rangle$. Therefore, the Boltzmann weight for each eigen-configuration \mathcal{C} is

$$\mathcal{W}_B(\mathcal{C}) = \exp(-\beta E_{\mathcal{C}}). \quad (5.3)$$

As we said before, diagonalization of H is a Herculean task, and the very existence of the current work can be traced to our attempt to dodge these difficulties as much as possible. Given the impossibility of solving the quantum system above, let us step back and scrutinize a classical counterpart of it.

Let us first observe that each eigen-configuration is composed as a sum of states classified by plane partitions, that is

$$|\Psi_{\mathcal{C}}\rangle = \sum_{\Lambda} \psi_{\mathcal{C}}(\Lambda, J, V, q) |\Lambda\rangle, \quad (5.4)$$

where each plane partition state corresponds to a Kagome lattice configuration. Consequently, each hexagon cell parametrized as in figure 10 gives a minute contribution to the partition function. With these observations, one could try a reverse engineering process: build eigenstates from sums of cell configurations products.

We want to understand the dynamics of these local configurations parametrized by the triads $Y^{(2a)}X^{(2a)}Y^{(2a-1)}$ or $Y^{(2a+1)}X^{(2a+1)}Y^{(2a)}$. Ultimately, we would like to assign Boltzmann to the

hexagons 10 and insert them back into the partition function expression; unfortunately, there is no natural way to assign statistical weights to each hexagon configuration. Throughout the remainder of this work we try to find functional relations for the Boltzmann weights imposed by integrability. As we show in a later section, we can suppose that these Boltzmann weights define two integrable subsystems related to vertex models.

Evidently, the associated classical problem is defined by a partition function of the form

$$Z_{cl} = \sum_{n_1, n_2, \dots} \prod_{\diamond} \mathcal{W}(\mathcal{C}, \diamond_i)^{n_i}, \quad (5.5)$$

where $\mathcal{W}(\mathcal{C}, \diamond)$ are local Boltzmann weights for each local configurations. We discuss this problem carefully next section. Hopefully, a better understanding of the classical system will unveil details of the quantum Hamiltonian (4.1a).

5.1 Local configurations

We define the local configurations that appear in the quantum problem, and using these allowed states, we define an associated classical statistical physics problem. Let us start with the local hexagon configuration represented by figure 10 with corresponding local state

$$|\diamond_{a,m}\rangle = \left| \begin{array}{cc} \mu_r^{(a)} & \mu_{r+1}^{(a)} \\ \alpha_m & \alpha_{m+2} \\ \mu_r^{(a-1)} & \mu_{r+1}^{(a-1)} \end{array} \right\rangle \quad \mu, \alpha \equiv \circ, \bullet. \quad (5.6)$$

Naïvely, there are $2^6 = 64$ such states, but since we are ultimately interested in the plane partition growth, there are constraints which send most of these configurations to zero. Let us start with these conditions.

Remember that there are two characteristic lattice distances: $d_Y = 1$, the lattice distance in the Y -spin chains, and $d_X = 2$ that is the lattice distance in the X -spin chain. Additionally, observe that the distance between a given site in the X -chain and the two nearest sites in the Y -spin chain is also $d_Y = 1$.

In the 0-box configuration $|\emptyset\rangle$, there is no nearest-neighbor pair of sites (those with $d_Y = 1$) occupied simultaneously by particles. In other words, given two sites with distance $= 1$, the configurations $|\bullet\bullet\rangle$ and $|\bullet\circ\rangle$ do not appear anywhere in the 0-box state. Using this *distance embargo*, we can get rid of many local hexagon states in the lattice. For example, local configurations in the two sets $\left\{ \left| \begin{smallmatrix} \bullet & \bullet \\ * & * \end{smallmatrix} \right\rangle \right\}$ and $\left\{ \left| \begin{smallmatrix} * & * \\ * & * \end{smallmatrix} \right\rangle \right\}$ are absent in $|\emptyset\rangle$. Similarly, states of the type $\left\{ \left| \begin{smallmatrix} \bullet & * \\ * & * \end{smallmatrix} \right\rangle \right\}$, $\left\{ \left| \begin{smallmatrix} * & \bullet \\ * & * \end{smallmatrix} \right\rangle \right\}$, $\left\{ \left| \begin{smallmatrix} * & * \\ \bullet & \bullet \end{smallmatrix} \right\rangle \right\}$ and $\left\{ \left| \begin{smallmatrix} * & * \\ * & \bullet \end{smallmatrix} \right\rangle \right\}$ are also forbidden. Finally, in the set $\left\{ \left| \begin{smallmatrix} * & * \\ \bullet & * \end{smallmatrix} \right\rangle \right\}$, only the state $\left| \begin{smallmatrix} \circ & \circ \\ \bullet & \bullet \\ \circ & \circ \end{smallmatrix} \right\rangle$ is allowed.

Observe that this restriction also forbids certain tensor product states. Making a list of all forbidden configurations is not a simple task anymore (and it is not necessary either), so let us understand the general idea with an example. Consider the product of two hexagons

$$|\diamond_{a,m}\rangle \otimes |\diamond_{a+1,m+2}\rangle = \left| \begin{array}{cc} \mu_r^{(a)} & \mu_{r+1}^{(a)} \\ \alpha_m & \alpha_{m+2} \\ \mu_r^{(a-1)} & \mu_{r+1}^{(a-1)} \end{array} \right\rangle \otimes \left| \begin{array}{cc} \mu_{r+1}^{(a+1)} & \mu_{r+2}^{(a+1)} \\ \alpha_{m+1} & \alpha_{m+3} \\ \mu_{r+1}^{(a)} & \mu_{r+2}^{(a)} \end{array} \right\rangle. \quad (5.7)$$

that we represent diagrammatically as in figure 11. It is easy to see that states in the set $\left\{ \left| \begin{smallmatrix} \bullet & * \\ * & * \end{smallmatrix} \right\rangle \otimes \left| \begin{smallmatrix} * & * \\ * & * \end{smallmatrix} \right\rangle \right\}$ are not allowed since $distance(\mu_r^{(a)}, \alpha_{m+1}) = d_Y = 1$.

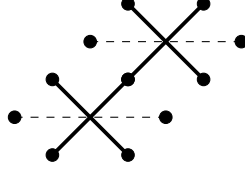


Figure 11: Diagrammatic representation of the tensor product state.

But now we need to ask ourselves if the absence of these states is a general feature or an artifact of the ground state. In order to answer this point, we need to understand some properties of the system we are interested in. First, observe that the Hamiltonian (4.1a) is written as a sum of local operators $H_{a,m}$ acting independently in each hexagon cell. There are just two states that give nontrivial results under its action, namely $\left\{ \left| \begin{smallmatrix} \circ & \circ \\ \bullet & \circ \end{smallmatrix} \right\rangle \right\}$ and $\left\{ \left| \begin{smallmatrix} \circ & \circ \\ \circ & \bullet \end{smallmatrix} \right\rangle \right\}$. As a matter of fact, the kinetic terms of $H_{a,m}$ exchange these two states whilst the potential term acts diagonally with eigenvalues 0 and 1. Therefore, if we consider the zero box state $|\emptyset\rangle$ as the ground state, the local states with nearest-neighbors are not generated in configurations corresponding to a generic plane partition. As an important remark, observe that the embargo above is a feature of the expansion around the zero box ground state.

From the restrictions above, the classification of the nontrivial hexagon states is just a simple combinatorics problem. There is, naturally, 1 empty hexagon state

$$\mathfrak{R}_0 = \left\{ |[0]\rangle \equiv \left| \begin{smallmatrix} \circ & \circ \\ \circ & \circ \end{smallmatrix} \right\rangle \right\}, \quad (5.8a)$$

and we have used the notation $|[n]_{abc}\rangle$, where n denotes the number of particles, and a, b, c their positions with relation to $\left| \begin{smallmatrix} 5 & 6 \\ 3 & 4 \\ 1 & 2 \end{smallmatrix} \right\rangle$. This notation will be clearer in the next example.

There are $6 = \binom{6}{1}$ states with 1 particle, and all of them are nontrivial, namely

$$\mathfrak{R}_1 = \left\{ \begin{aligned} |[1]_1\rangle &\equiv \left| \begin{smallmatrix} \circ & \circ \\ \bullet & \circ \end{smallmatrix} \right\rangle; & |[1]_2\rangle &\equiv \left| \begin{smallmatrix} \circ & \circ \\ \circ & \bullet \end{smallmatrix} \right\rangle; & |[1]_3\rangle &\equiv \left| \begin{smallmatrix} \circ & \bullet \\ \circ & \circ \end{smallmatrix} \right\rangle \\ |[1]_4\rangle &\equiv \left| \begin{smallmatrix} \circ & \bullet \\ \bullet & \circ \end{smallmatrix} \right\rangle; & |[1]_5\rangle &\equiv \left| \begin{smallmatrix} \bullet & \circ \\ \circ & \circ \end{smallmatrix} \right\rangle; & |[1]_6\rangle &\equiv \left| \begin{smallmatrix} \circ & \circ \\ \circ & \bullet \end{smallmatrix} \right\rangle \end{aligned} \right\}. \quad (5.8b)$$

Furthermore, we have $15 = \binom{6}{2}$ states with 2 particles, and 9 of them are nontrivial, namely

$$\mathfrak{R}_2 = \left\{ \begin{aligned} |[2]_{14}\rangle &\equiv \left| \begin{smallmatrix} \circ & \circ \\ \bullet & \bullet \end{smallmatrix} \right\rangle; & |[2]_{15}\rangle &\equiv \left| \begin{smallmatrix} \bullet & \circ \\ \bullet & \circ \end{smallmatrix} \right\rangle; & |[2]_{16}\rangle &\equiv \left| \begin{smallmatrix} \circ & \bullet \\ \bullet & \circ \end{smallmatrix} \right\rangle \\ |[2]_{23}\rangle &\equiv \left| \begin{smallmatrix} \circ & \circ \\ \bullet & \bullet \end{smallmatrix} \right\rangle; & |[2]_{25}\rangle &\equiv \left| \begin{smallmatrix} \bullet & \circ \\ \circ & \bullet \end{smallmatrix} \right\rangle; & |[2]_{26}\rangle &\equiv \left| \begin{smallmatrix} \circ & \bullet \\ \circ & \bullet \end{smallmatrix} \right\rangle \\ |[2]_{34}\rangle &\equiv \left| \begin{smallmatrix} \circ & \bullet \\ \bullet & \circ \end{smallmatrix} \right\rangle; & |[2]_{36}\rangle &\equiv \left| \begin{smallmatrix} \bullet & \circ \\ \circ & \circ \end{smallmatrix} \right\rangle; \\ |[2]_{45}\rangle &\equiv \left| \begin{smallmatrix} \bullet & \bullet \\ \circ & \circ \end{smallmatrix} \right\rangle \end{aligned} \right\} \quad (5.8c)$$

There are $20 = \binom{6}{3}$ with 3 particles, and 2 of them are relevant to our discussion, namely

$$\mathfrak{R}_3 = \left\{ |[3]_{236}\rangle \equiv \left| \begin{smallmatrix} \circ & \bullet \\ \bullet & \bullet \end{smallmatrix} \right\rangle; |[3]_{145}\rangle \equiv \left| \begin{smallmatrix} \bullet & \circ \\ \bullet & \circ \end{smallmatrix} \right\rangle \right\}, \quad (5.8d)$$

and all other states are null.

Finally, there is just 1 state with 6 particles, $6 = \binom{6}{5}$ states with 5 particles, and $15 = \binom{6}{4}$ states with 4 particles. All these states are null since there are necessarily two particles occupying nearest-neighbor sites.

Putting all these facts together, we immediately see that there are 18 nontrivial states. We should remark that, in principle, there is absolutely nothing wrong with the null states above, they simply do not appear in the system we are interested in. The set of physical hexagon states is

$$\mathfrak{R} = \mathfrak{R}_0 \cup \mathfrak{R}_1 \cup \mathfrak{R}_2 \cup \mathfrak{R}_3 . \quad (5.9)$$

5.2 Macroscopic configurations & Classical statistical system

The rules to consistently combine local states to create macroscopic configurations \mathcal{C} are defined now. In fact, we have already considered the X and Y -rows parametrization, thus we know how to do connect the hexagons consistently; but now we want to put in words the rules we have been using. From the parametrization of figure 10, the consistent configurations are obtained with the following rules:

Rules

- Consider two hexagons A and B in the triad $Y^{(a-1)}X^{(a)}Y^{(a)}$ and generic parametrization (a, m) and (a, m') respectively. They are connected horizontally if one of the following conditions is satisfied:

$$\text{Rule \#1: } \alpha_{m+2}^A = \alpha_{m'}^B \quad \text{for } m+2 = m' \quad (5.10a)$$

$$\text{Rule \#2: } \alpha_m^A = \alpha_{m'+2}^B \quad \text{for } m = m' + 2 . \quad (5.10b)$$

- Consider a hexagon A in the triad $Y^{(a-1)}X^{(a)}Y^{(a)}$ parametrized by (a, m) , and another hexagon B in the triad $Y^{(a)}X^{(a+1)}Y^{(a+1)}$ parametrized by $(a+1, m')$. They are connected diagonally if one of the following conditions is satisfied:

$$\text{Rule \#3: } \mu_{m+3/2}^{A(a)} = \mu_{m'+1/2}^{B(a)} \quad \text{for } m+1 = m' \quad (5.10c)$$

$$\text{Rule \#4: } \mu_{m+1/2}^{A(a)} = \mu_{m'+3/2}^{B(a)} \quad \text{for } m = m' + 1 . \quad (5.10d)$$

Using the rules above repeatedly, we can build the macroscopic configurations \mathcal{C} , and counting these possible \mathcal{C} is the essence of the classical statistical problem we want to study. It should also be clear now that the vast majority of the consistent configurations \mathcal{C} do not define plane partitions configurations. In particular, we do not impose any restriction on particles occupying sites with distance = 1. Evidently, at some point we need to impose this extra layer of complexity, but now we are interested in this simplified classical problem.

Given a macroscopic configuration \mathcal{C} , its Boltzmann weight is defined by $\mathcal{W}(\mathcal{C})$, and since it is a combination of the 18 hexagon states we defined before, we write

$$\mathcal{W}(\mathcal{C}) = \prod_{i=1}^{18} \mathcal{W}(\mathcal{C}, \diamond_i) \quad (5.11)$$

where \mathcal{C} is defined by a string of integers $\vec{n} = \{n_1, n_2, \dots, n_{18}\}$ which determines how many times the hexagon \diamond_i appears in \mathcal{C} . Moreover, if we write $\mathcal{W}(1, \diamond_i) = \exp(-\beta \varepsilon_i)$, the classical partition

function (5.5) reads

$$Z_{cl} = \sum_{\vec{n}} \exp \left(-\beta \sum_{i=1}^{18} n_i \varepsilon_i \right). \quad (5.12)$$

We can denote diagrammatically the hexagon configurations as in figure 12. In section 6 we show that integrability of this system cannot be settled using a naïve row-to-row formalism, but with small modification of the rules (5.10a – 5.10d), we can make contact between this model and a descendant of the 6-vertex model. We need to remark that albeit the similarities, the statistical system above does not define an ordinary vertex model since the thick lines can finish within the lattice configuration \mathcal{C} , and not just at the boundaries.

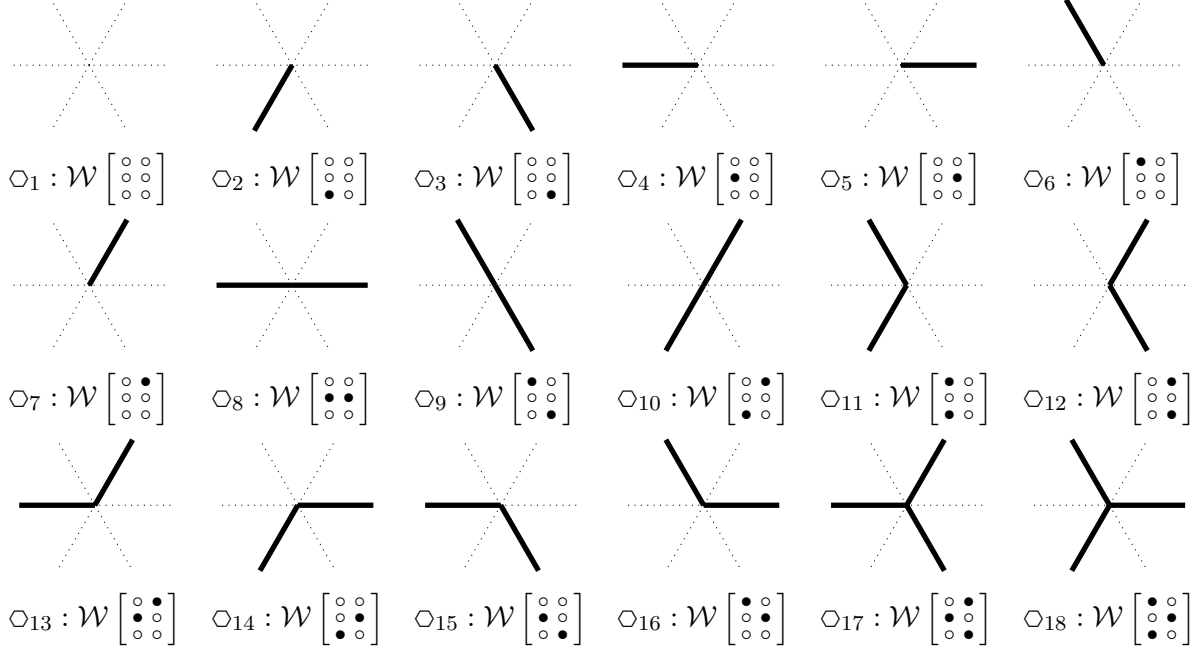


Figure 12: 18 hexagon vertex configurations with their respective weights.

5.3 Lax operator

In this section, we decompose each hexagon cell in three incoming and three outgoing particles, as in figure 13, to define an S-matrix, that we recklessly call Lax operator. From the S-matrix expressions, we define the Boltzmann weights to be the scattering amplitudes of these processes. See [16] for an example of this idea in the 6- and 8-vertex models.

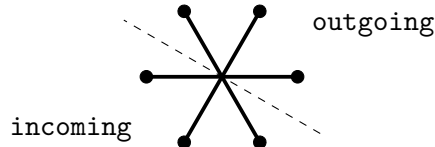


Figure 13: Scattering process

In principle, there 64 different processes of the type represented by figure 13 with 8 incoming and 8 outgoing different configurations each. But as we said before, there are several forbidden

configurations. From the diagrams 12, it is easy to see that there are just 5 incoming and 5 outgoing nontrivial configurations

$$\begin{aligned} \text{incoming} &= \{|\circ\circ\rangle, |\bullet\circ\rangle, |\bullet\bullet\rangle, |\circ\bullet\rangle, |\bullet\bullet\rangle\} \\ \text{outgoing} &= \{|\circ\circ\rangle, |\bullet\circ\rangle, |\bullet\bullet\rangle, |\circ\bullet\rangle, |\bullet\bullet\rangle\}. \end{aligned} \quad (5.13)$$

In other words, the initial $|\bullet\circ\rangle, |\circ\bullet\rangle, |\bullet\bullet\rangle$ and final $|\circ\bullet\rangle, |\bullet\circ\rangle, |\bullet\bullet\rangle$ states decouple from the space of physical states, see figure 14.

Let us denote the Hilbert space associated to the $X^{(a)}$ -chains by $\tilde{\mathcal{H}}^{(a)} = \bigotimes_m \tilde{V}_m^{(a)}$ and the one associated to the $Y^{(a)}$ -chains by $\mathcal{H}^{(a)} = \bigotimes_r V_r^{(a)}$, where $\tilde{V}_m \simeq V_r \simeq \mathbb{C}^2$. The space $\tilde{V} \simeq \mathbb{C}^2$ is called the *auxiliary* or *horizontal* space, and $V \times V \simeq \mathbb{C}^4$ the *quantum* or *vertical* space.

The Lax operator $\mathcal{L}_{a,m}$ is then defined as

$$\mathcal{L}_{a,m} : \tilde{V}_m^{(a)} \otimes V_{m+1/2}^{(a-1)} \otimes V_{m+3/2}^{(a-1)} \rightarrow \tilde{V}_{m+2}^{(a)} \otimes V_{m+1/2}^{(a)} \otimes V_{m+3/2}^{(a)}, \quad (5.14)$$

with action

$$\mathcal{L}_{a,m} |\alpha_{\mu_1} \mu_2\rangle = \sum_{\beta, \nu_1, \nu_2} \mathcal{W} \begin{bmatrix} \nu_1 & \nu_2 \\ \alpha & \beta \\ \mu_1 & \mu_2 \end{bmatrix} |\nu_1 \nu_2\rangle, \quad (5.15)$$

where $\mathcal{W} \begin{bmatrix} \nu_1 & \nu_2 \\ \alpha & \beta \\ \mu_1 & \mu_2 \end{bmatrix}$ is the Boltzmann weight associated to a state parametrized accordingly. Therefore

$$\begin{aligned} \mathcal{L}_{a,m} |\circ\circ\rangle &= \mathcal{W} \begin{bmatrix} \circ & \circ \\ \circ & \circ \\ \circ & \circ \end{bmatrix} |\circ\circ\rangle + \mathcal{W} \begin{bmatrix} \circ & \circ \\ \bullet & \circ \\ \circ & \circ \end{bmatrix} |\bullet\circ\rangle + \mathcal{W} \begin{bmatrix} \circ & \circ \\ \circ & \bullet \\ \circ & \circ \end{bmatrix} |\circ\bullet\rangle + \mathcal{W} \begin{bmatrix} \circ & \circ \\ \circ & \circ \\ \bullet & \bullet \end{bmatrix} |\bullet\bullet\rangle \\ \mathcal{L}_{a,m} |\bullet\circ\rangle &= \mathcal{W} \begin{bmatrix} \circ & \circ \\ \bullet & \circ \\ \bullet & \circ \end{bmatrix} |\circ\circ\rangle + \mathcal{W} \begin{bmatrix} \circ & \circ \\ \bullet & \circ \\ \bullet & \bullet \end{bmatrix} |\bullet\circ\rangle + \mathcal{W} \begin{bmatrix} \circ & \circ \\ \circ & \bullet \\ \bullet & \circ \end{bmatrix} |\circ\bullet\rangle + \mathcal{W} \begin{bmatrix} \circ & \circ \\ \bullet & \circ \\ \bullet & \bullet \end{bmatrix} |\bullet\bullet\rangle \\ \mathcal{L}_{a,m} |\circ\bullet\rangle &= \mathcal{W} \begin{bmatrix} \circ & \circ \\ \circ & \bullet \\ \circ & \bullet \end{bmatrix} |\circ\circ\rangle + \mathcal{W} \begin{bmatrix} \circ & \circ \\ \bullet & \bullet \\ \circ & \bullet \end{bmatrix} |\bullet\circ\rangle + \mathcal{W} \begin{bmatrix} \circ & \circ \\ \circ & \bullet \\ \bullet & \bullet \end{bmatrix} |\circ\bullet\rangle \\ \mathcal{L}_{a,m} |\bullet\bullet\rangle &= \mathcal{W} \begin{bmatrix} \circ & \circ \\ \bullet & \bullet \\ \bullet & \bullet \end{bmatrix} |\circ\circ\rangle + \mathcal{W} \begin{bmatrix} \circ & \circ \\ \bullet & \bullet \\ \bullet & \bullet \end{bmatrix} |\bullet\circ\rangle + \mathcal{W} \begin{bmatrix} \circ & \circ \\ \circ & \bullet \\ \bullet & \bullet \end{bmatrix} |\circ\bullet\rangle \\ \mathcal{L}_{a,m} |\bullet\bullet\rangle &= \mathcal{W} \begin{bmatrix} \circ & \circ \\ \bullet & \bullet \\ \bullet & \bullet \end{bmatrix} |\circ\circ\rangle + \mathcal{W} \begin{bmatrix} \circ & \circ \\ \bullet & \bullet \\ \bullet & \bullet \end{bmatrix} |\bullet\circ\rangle \end{aligned} \quad (5.16)$$

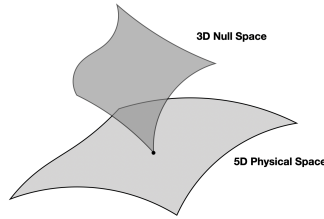


Figure 14: Physical and null spaces.

In other words, the most general Lax operator is given by

$$\mathcal{L}_{a,m} = \begin{pmatrix} \langle \begin{smallmatrix} \circ & \circ \\ \bullet & \circ \end{smallmatrix} | \mathcal{L}_{a,m} | \begin{smallmatrix} \circ & \circ \\ \circ & \circ \end{smallmatrix} \rangle & \langle \begin{smallmatrix} \circ & \circ \\ \bullet & \circ \end{smallmatrix} | \mathcal{L}_{a,m} | \begin{smallmatrix} \circ & \circ \\ \circ & \bullet \end{smallmatrix} \rangle & \langle \begin{smallmatrix} \circ & \circ \\ \bullet & \circ \end{smallmatrix} | \mathcal{L}_{a,m} | \begin{smallmatrix} \circ & \circ \\ \circ & \bullet \end{smallmatrix} \rangle & \langle \begin{smallmatrix} \circ & \circ \\ \bullet & \circ \end{smallmatrix} | \mathcal{L}_{a,m} | \begin{smallmatrix} \circ & \circ \\ \bullet & \circ \end{smallmatrix} \rangle & \langle \begin{smallmatrix} \circ & \circ \\ \bullet & \circ \end{smallmatrix} | \mathcal{L}_{a,m} | \begin{smallmatrix} \circ & \circ \\ \bullet & \bullet \end{smallmatrix} \rangle \\ \langle \begin{smallmatrix} \circ & \circ \\ \bullet & \circ \end{smallmatrix} | \mathcal{L}_{a,m} | \begin{smallmatrix} \circ & \circ \\ \circ & \circ \end{smallmatrix} \rangle & \langle \begin{smallmatrix} \circ & \circ \\ \bullet & \circ \end{smallmatrix} | \mathcal{L}_{a,m} | \begin{smallmatrix} \circ & \circ \\ \circ & \bullet \end{smallmatrix} \rangle & \langle \begin{smallmatrix} \circ & \circ \\ \bullet & \circ \end{smallmatrix} | \mathcal{L}_{a,m} | \begin{smallmatrix} \circ & \circ \\ \circ & \bullet \end{smallmatrix} \rangle & \langle \begin{smallmatrix} \circ & \circ \\ \bullet & \circ \end{smallmatrix} | \mathcal{L}_{a,m} | \begin{smallmatrix} \circ & \circ \\ \bullet & \circ \end{smallmatrix} \rangle & \langle \begin{smallmatrix} \circ & \circ \\ \bullet & \circ \end{smallmatrix} | \mathcal{L}_{a,m} | \begin{smallmatrix} \circ & \circ \\ \bullet & \bullet \end{smallmatrix} \rangle \\ \langle \begin{smallmatrix} \circ & \circ \\ \bullet & \circ \end{smallmatrix} | \mathcal{L}_{a,m} | \begin{smallmatrix} \circ & \circ \\ \circ & \circ \end{smallmatrix} \rangle & \langle \begin{smallmatrix} \circ & \circ \\ \bullet & \circ \end{smallmatrix} | \mathcal{L}_{a,m} | \begin{smallmatrix} \circ & \circ \\ \circ & \bullet \end{smallmatrix} \rangle & \langle \begin{smallmatrix} \circ & \circ \\ \bullet & \circ \end{smallmatrix} | \mathcal{L}_{a,m} | \begin{smallmatrix} \circ & \circ \\ \circ & \bullet \end{smallmatrix} \rangle & \langle \begin{smallmatrix} \circ & \circ \\ \bullet & \circ \end{smallmatrix} | \mathcal{L}_{a,m} | \begin{smallmatrix} \circ & \circ \\ \bullet & \circ \end{smallmatrix} \rangle & \langle \begin{smallmatrix} \circ & \circ \\ \bullet & \circ \end{smallmatrix} | \mathcal{L}_{a,m} | \begin{smallmatrix} \circ & \circ \\ \bullet & \bullet \end{smallmatrix} \rangle \\ \langle \begin{smallmatrix} \circ & \circ \\ \bullet & \circ \end{smallmatrix} | \mathcal{L}_{a,m} | \begin{smallmatrix} \circ & \circ \\ \circ & \circ \end{smallmatrix} \rangle & \langle \begin{smallmatrix} \circ & \circ \\ \bullet & \circ \end{smallmatrix} | \mathcal{L}_{a,m} | \begin{smallmatrix} \circ & \circ \\ \circ & \bullet \end{smallmatrix} \rangle & \langle \begin{smallmatrix} \circ & \circ \\ \bullet & \circ \end{smallmatrix} | \mathcal{L}_{a,m} | \begin{smallmatrix} \circ & \circ \\ \circ & \bullet \end{smallmatrix} \rangle & \langle \begin{smallmatrix} \circ & \circ \\ \bullet & \circ \end{smallmatrix} | \mathcal{L}_{a,m} | \begin{smallmatrix} \circ & \circ \\ \bullet & \circ \end{smallmatrix} \rangle & \langle \begin{smallmatrix} \circ & \circ \\ \bullet & \circ \end{smallmatrix} | \mathcal{L}_{a,m} | \begin{smallmatrix} \circ & \circ \\ \bullet & \bullet \end{smallmatrix} \rangle \end{pmatrix} \mathbf{0}_{3 \times 3} \quad (5.17a)$$

where the nonsingular 5×5 matrix reads

$$\mathcal{L}_{a,m}^{(5 \times 5)} = \begin{pmatrix} \mathcal{W}([0]) & \mathcal{W}([1]_2) & \mathcal{W}([1]_1) & \mathcal{W}([1]_3) & \mathcal{W}([2]_{23}) \\ \mathcal{W}([1]_5) & \mathcal{W}([2]_{25}) & \mathcal{W}([2]_{15}) & 0 & 0 \\ \mathcal{W}([1]_6) & \mathcal{W}([2]_{26}) & \mathcal{W}([2]_{16}) & \mathcal{W}([2]_{36}) & \mathcal{W}([3]_{236}) \\ \mathcal{W}([1]_4) & 0 & \mathcal{W}([2]_{14}) & \mathcal{W}([2]_{34}) & 0 \\ \mathcal{W}([2]_{45}) & 0 & \mathcal{W}([3]_{145}) & 0 & 0 \end{pmatrix}. \quad (5.17b)$$

As we explained before, we would like to see this operator as an S -matrix. Remember that the physical space (defined by the incoming or outgoing vectors (5.13)) is 5 dimensional, and the other 3 directions decouple from the scattering process. Therefore, the fact that $\mathcal{L}_{a,m}$ is a singular matrix is just a spurious result of our insistence in writing it with its legs along the 3D null space, see 14. As we see next section, there are some advantages in considering these terms.

One important aspect we have ignored so far is the dependence of all Boltzmann weights on the parameters J, V and q . We can now suppose that these constants depend on the spectral parameter u , that is $J = J(u), V = V(u)$ and $q = q(u)$, therefore the Boltzmann weights can also be denoted as

$$\mathcal{W} \begin{bmatrix} \nu_1 & \nu_2 \\ \alpha & \beta \\ \mu_1 & \mu_2 \end{bmatrix} \equiv \mathcal{W} \left[u \middle| \begin{smallmatrix} \nu_1 & \nu_2 \\ \alpha & \beta \\ \mu_1 & \mu_2 \end{smallmatrix} \right]. \quad (5.18)$$

In order to simplify the notation, we will keep the dependence on the spectral parameter implicit, and we reintroduce its dependence conveniently, for example, in the expression for *row-to-row transfer matrix* that we define now

$$\mathbf{t}_a(u) = \text{Tr}_{\mathcal{H}^{(a)}} \left(\prod_m \mathcal{L}_{a,m}(u) \right). \quad (5.19)$$

As usual, we can think of it as an operator that transfers the state $|\mu\rangle \in \mathcal{H}^{(a-1)}$ to a linear combination of $|\nu\rangle \in \mathcal{H}^{(a)}$. More specifically

$$\mathbf{t}_a|\mu\rangle = \sum_{\nu} (\mathbf{T}_a)_{\mu}^{\nu} |\nu\rangle \quad (5.20a)$$

where

$$\begin{aligned} |\mu\rangle &= |\mu_1, \tilde{\mu}_1, \mu_2, \tilde{\mu}_2, \dots, \mu_N, \tilde{\mu}_N\rangle \\ |\nu\rangle &= |\nu_1, \tilde{\nu}_1, \mu_2, \tilde{\nu}_2, \dots, \nu_N, \tilde{\nu}_N\rangle, \end{aligned} \quad (5.20b)$$

and

$$(\mathbf{t}_a)_{\mu}^{\nu} = \langle \nu | \mathbf{T}_a | \mu \rangle = \sum_{\alpha} \mathcal{W} \begin{bmatrix} \nu_1 & \tilde{\nu}_1 \\ \alpha_1 & \alpha_2 \\ \mu_1 & \tilde{\mu}_1 \end{bmatrix} \mathcal{W} \begin{bmatrix} \nu_2 & \tilde{\nu}_2 \\ \alpha_2 & \alpha_3 \\ \mu_2 & \tilde{\mu}_3 \end{bmatrix} \dots \mathcal{W} \begin{bmatrix} \nu_{N-1} & \tilde{\nu}_{N-1} \\ \alpha_{N-1} & \alpha_N \\ \mu_{N-1} & \tilde{\mu}_{N-1} \end{bmatrix} \mathcal{W} \begin{bmatrix} \nu_N & \tilde{\nu}_N \\ \alpha_N & \alpha_1 \\ \mu_N & \tilde{\mu}_N \end{bmatrix}. \quad (5.20c)$$

We have more to say about the transfer matrix next section.

6 Integrable (sub-) systems & Vertex models

We have implicitly assumed that the hexagons weights do not depend on their parametrization – the position (a, m) in the lattice – but depend on the position and number of particles inside the hexagon. This hypothesis allowed us to define the weights of figure 12 regardless of their particular location in the lattice. On the other hand, we need to be precise on the parametrization since the relative hexagon positions change from even to odd rows. This also implies that we actually have two types of Lax operators (5.15), namely

$$\mathcal{L}_{2a,2m} : \tilde{V}_{2m}^{(2a)} \otimes V_{2m+1/2}^{(2a-1)} \otimes V_{2m+3/2}^{(2a-1)} \rightarrow \tilde{V}_{2m+2}^{(2a)} \otimes V_{2m+1/2}^{(2a)} \otimes V_{2m+3/2}^{(2a)} \quad (6.1a)$$

and

$$\mathcal{L}_{2a+1,2m+1} : \tilde{V}_{2m+1}^{(2a+1)} \otimes V_{2m+3/2}^{(2a)} \otimes V_{2m+5/2}^{(2a)} \rightarrow \tilde{V}_{2m+3}^{(2a+1)} \otimes V_{2m+3/2}^{(2a+1)} \otimes V_{2m+5/2}^{(2a+1)} . \quad (6.1b)$$

Observe that our parametrization does not allow operators of the form $\mathcal{L}_{2a,2m+1}$ or $\mathcal{L}_{2a+1,2m}$. Evidently, since all these vector spaces are isomorphic the flamboyant notation above is unnecessary and we can simply write $\mathcal{L}_{2a,2m}, \mathcal{L}_{2a+1,2m+1} \in \text{End}(\tilde{V} \otimes V^2)$. Consequently, there are two types of row-to-row transfer matrices

$$\begin{aligned} t(u) &= \text{Tr}_{\tilde{\mathcal{H}}(2a)} \left(\prod_m \mathcal{L}_{2a,2m}(u) \right) \\ \tilde{t}(u) &= \text{Tr}_{\tilde{\mathcal{H}}(2a+1)} \left(\prod_m \mathcal{L}_{2a+1,2m+1}(u) \right) . \end{aligned} \quad (6.2)$$

As we said before, the system has M -columns (where we count by the number of hexagons), which means that there are $2M$ slots in the X- and Y-rows. Remember that we have also imposed periodic boundary conditions, $2M \sim 0$. Therefore, the transfer matrices act as

$$t|\mu_{1/2}\mu_{3/2} \cdots \mu_{2M-3/2}\mu_{2M-1/2}\rangle = \sum_{\nu} t_{\mu_{1/2}\mu_{3/2} \cdots \mu_{2M-3/2}\mu_{2M-1/2}}^{\nu_{1/2}\nu_{3/2} \cdots \nu_{2M-3/2}\nu_{2M-1/2}} |\nu_{1/2}\nu_{3/2} \cdots \nu_{2M-3/2}\nu_{2M-1/2}\rangle , \quad (6.3a)$$

and

$$\begin{aligned} \tilde{t}|\nu_{1/2}\nu_{3/2} \cdots \nu_{2M-3/2}\nu_{2M-1/2}\rangle &\equiv \tilde{t}|\nu_{3/2}\nu_{5/2} \cdots \nu_{2M-1/2}\nu_{2M+1/2}\rangle \\ &= \sum_{\mu'} \tilde{t}_{\nu_{3/2}\nu_{5/2} \cdots \nu_{2M-1/2}\nu_{2M+1/2}}^{\mu'_{3/2}\mu'_{5/2} \cdots \mu'_{2M-1/2}\mu'_{2M+1/2}} |\mu'_{3/2}\mu'_{5/2} \cdots \mu'_{2M-1/2}\mu'_{2M+1/2}\rangle , \end{aligned} \quad (6.3b)$$

where we have used that $2M + 1/2 \sim 1/2$ and $2M + 1 \sim 1$. Finally, the transfer matrices components can be easily calculated

$$t_{\mu_{1/2}\mu_{3/2} \cdots \mu_{2M-3/2}\mu_{2M-1/2}}^{\nu_{1/2}\nu_{3/2} \cdots \nu_{2M-3/2}\nu_{2M-1/2}} = \sum_{\alpha} \mathcal{W} \begin{bmatrix} \nu_{1/2} & \nu_{3/2} \\ \alpha_0 & \alpha_2 \\ \mu_{1/2} & \mu_{3/2} \end{bmatrix} \mathcal{W} \begin{bmatrix} \nu_{5/2} & \nu_{7/2} \\ \alpha_2 & \alpha_4 \\ \mu_{5/2} & \mu_{7/2} \end{bmatrix} \cdots \mathcal{W} \begin{bmatrix} \nu_{2M-3/2} & \nu_{2M-1/2} \\ \alpha_{2M} & \alpha_0 \\ \mu_{2M-3/2} & \mu_{2M-1/2} \end{bmatrix} \quad (6.4a)$$

and

$$\tilde{t}_{\nu_{3/2}\nu_{5/2} \cdots \nu_{2M-1/2}\nu_{2M+1/2}}^{\mu'_{3/2}\mu'_{5/2} \cdots \mu'_{2M-1/2}\mu'_{2M+1/2}} = \sum_{\alpha} \mathcal{W} \begin{bmatrix} \mu'_{3/2} & \mu'_{5/2} \\ \alpha_1 & \alpha_3 \\ \nu_{3/2} & \nu_{5/2} \end{bmatrix} \mathcal{W} \begin{bmatrix} \mu'_{7/2} & \mu'_{9/2} \\ \alpha_3 & \alpha_5 \\ \nu_{7/2} & \nu_{9/2} \end{bmatrix} \cdots \mathcal{W} \begin{bmatrix} \mu'_{2M-1/2} & \mu'_{1/2} \\ \alpha_{2M-1} & \alpha_1 \\ \nu_{2M-1/2} & \nu_{1/2} \end{bmatrix} . \quad (6.4b)$$

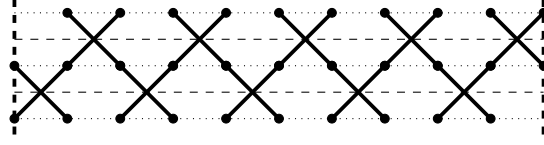


Figure 15: Transfer matrices product $\mathbf{t} \tilde{\mathbf{t}}$ for $M = 5$.

6.1 Transfer matrices commutation relations

With this knowledge, we would like to study commutation relations of the transfer matrices. It is well known that for a generic integrable system, the conserved quantities I_n are obtained from an expansion of the form $\ln t(u) = \sum_n I_n u^n$ where $t(u)$ is the transfer matrix. Finally, the commutativity of I_n is a consequence of the generalized commutation relation $[t(u), t(v)] = 0$.

Using the transfer matrices we have defined above, one can ask if their existence implies the integrability of the classical statistical problem we have defined. The answer turns out to be no, but in an interesting and promising way. Let us start with the products

$$\mathbf{t} \mathbf{t}' = \text{Tr}_{\tilde{\mathcal{H}}^{(2a)} \times \tilde{\mathcal{H}}^{(2b)}} (\mathcal{L}_{2a,0} \mathcal{L}'_{2b,0} \mathcal{L}_{2a,1} \mathcal{L}'_{2b,1} \cdots \mathcal{L}_{2a,2M-2} \mathcal{L}'_{2b,2M-2}) \quad (6.5)$$

and

$$\mathbf{t}' \mathbf{t} = \text{Tr}_{\tilde{\mathcal{H}}^{(2b)} \times \tilde{\mathcal{H}}^{(2a)}} (\mathcal{L}'_{2b,0} \mathcal{L}_{2a,0} \mathcal{L}'_{2b,1} \mathcal{L}_{2a,1} \cdots \mathcal{L}'_{2b,2M-2} \mathcal{L}_{2a,2M-2}) \quad (6.6)$$

where $\mathbf{t} \equiv \mathbf{t}(u)$ and $\mathbf{t}' \equiv \mathbf{t}(v)$. It is easy to see that these two expressions are equal if there exists an operator \mathcal{R} such that

$$\boxed{\mathcal{R}_{2a,2b} \mathcal{L}_{2a,2m} \mathcal{L}'_{2b,2m} \stackrel{!}{=} \mathcal{L}'_{2b,2m} \mathcal{L}_{2a,2m} \mathcal{R}_{2a,2b}} \quad (6.7)$$

Similarly, one can show that $[\tilde{\mathbf{t}}, \tilde{\mathbf{t}}'] = 0$ iff

$$\boxed{\mathcal{R}_{2a+1,2b+1} \mathcal{L}_{2a+1,2m+1} \mathcal{L}'_{2b+1,2m+1} \stackrel{!}{=} \mathcal{L}'_{2b+1,2m+1} \mathcal{L}_{2a+1,2m+1} \mathcal{R}_{2a+1,2b+1}} \quad (6.8)$$

The case $[\mathbf{t}(u), \tilde{\mathbf{t}}(v)]$ is more interesting. The product can be diagrammatically represented in figure 15, where the vertical lines denote periodic boundary condition. Observe that

$$\tilde{\mathbf{t}} \mathbf{t} = \text{Tr}_{\tilde{\mathcal{H}}^{(2b+1)} \times \tilde{\mathcal{H}}^{(2a)}} (\mathcal{L}_{2b+1,1} \mathcal{L}_{2a,0} \mathcal{L}_{2b+1,3} \mathcal{L}_{2a,2} \mathcal{L}_{2b+1,5} \mathcal{L}_{2a,4} \cdots \mathcal{L}_{2b+1,2M-1} \mathcal{L}_{2a,2M-2}) \quad (6.9)$$

and

$$\mathbf{t} \tilde{\mathbf{t}} = \text{Tr}_{\tilde{\mathcal{H}}^{(2a)} \times \tilde{\mathcal{H}}^{(2b+1)}} (\mathcal{L}_{2a,0} \mathcal{L}_{2a,2} \mathcal{L}_{2b+1,1} \mathcal{L}_{2a,4} \mathcal{L}_{2b+1,3} \cdots \mathcal{L}_{2a,2M-2} \mathcal{L}_{2a,2M-3} \mathcal{L}_{2b+1,2M-1}) \quad (6.10)$$

The expressions above are not equal since the commutators $[\mathcal{L}_{a,m}, \mathcal{L}_{b,n}]$ do not necessarily vanish for $m \neq n$. In fact, it is easy to see that for states with corresponding diagrams 11, we have $[\mathcal{L}_{a,m}, \mathcal{L}_{a+1,m+1}] \neq 0$ and $[\mathcal{L}_{a,m}, \mathcal{L}_{a+1,m'}] = 0$ for $m' > m + 1$. Therefore, we have

$$[\mathbf{t}(u), \tilde{\mathbf{t}}(v)] \neq 0, \quad (6.11)$$

which spoils the naïve integrability of the classical statistical system we are considering. It is worth stressing that this non-commutativity does not disprove integrable, it just say that the row-to-row transfer matrix above is not appropriate. In summary, it is possible that the system is, indeed, non-integrable, but we have not yet ruled out its integrability.

6.2 Integrability for even and odd subsystems

Observe that the commutation relations for the even and odd transfer matrices (6.7) and (6.8) satisfy the properties we are looking for. We want to finish this work explaining how subsystems defined by even or odd rows are connected to vertex models.

We first modify the rules (5.10a), (5.10b), (5.10c) and (5.10d) defined in section 5.2. We still assume the same set of local configurations of figures 12, but now we connect them using the following rules

Rules

- Consider two hexagons A and B in the triad $Y^{(a-1)}X^{(a)}Y^{(a)}$, with generic parametrization (a, m) and (a, m') respectively. They are connected horizontally if one of the following conditions is satisfied:

$$\text{Rule \#1 : } \alpha_{m+2}^A = \alpha_{m'}^B \quad \text{for } m+2 = m' \quad (6.12a)$$

$$\text{Rule \#2 : } \alpha_m^A = \alpha_{m'+2}^B \quad \text{for } m = m' + 2. \quad (6.12b)$$

- Consider a hexagon A in the triad $Y^{(a-1)}X^{(a)}Y^{(a)}$ parametrized by (a, m) , and another hexagon B in the triad $Y^{(a)}X^{(a+1)}Y^{(a+1)}$ parametrized by $(a+1, m')$. They are connected vertically if the following conditions are satisfied:

$$\text{Rule \#5 : } \mu_{m+1/2}^{A(a)} = \mu_{m'+1/2}^{B(a)} \quad \text{for } m = m' \quad (6.12c)$$

$$\text{Rule \#6 : } \mu_{m+3/2}^{A(a)} = \mu_{m'+3/2}^{B(a)} \quad \text{for } m = m'. \quad (6.12d)$$

In other words, we have not changed the rules (5.10a), (5.10b), but now we link the rows vertically and not diagonally. It should be clear that in this case we do not have a Kagome lattice anymore, instead, we consider a triangular tiling of the plane. With these rules, the even and odd rows are completely equivalent, so we can consider simultaneously. Therefore, one can write (6.7) and (6.8) as

$$\boxed{\mathcal{R}_{a,b}(u, v) \mathcal{L}_{a,m}(u) \mathcal{L}_{b,m}(v) = \mathcal{L}_{b,m}(v) \mathcal{L}_{a,m}(u) \mathcal{R}_{a,b}(u, v)}, \quad (6.13)$$

that is known as the *fundamental commutation relation* (fcc).

Since integrability is a global property, we need to show the implications of these relations on the monodromy matrices. Let us consider a right multiplication of (6.13) by $\mathcal{L}_{a,m+1} \mathcal{L}'_{b,m+1}$, then

$$\begin{aligned} \mathcal{R}_{a,b} \mathcal{L}_{a,m} \mathcal{L}'_{b,m} \mathcal{L}_{a,m+1} \mathcal{L}'_{b,m+1} &= \mathcal{L}'_{b,m} \mathcal{L}_{a,m} \mathcal{R}_{a,b} \mathcal{L}_{a,m+1} \mathcal{L}'_{b,m+1} \\ &= \mathcal{L}'_{b,m} \mathcal{L}_{a,m} \mathcal{L}'_{b,m+1} \mathcal{L}_{a,m+1} \mathcal{R}_{a,b} \end{aligned} \quad (6.14a)$$

where we use (6.7) or (6.8) in the second line. Additionally, ultralocality implies

$$\mathcal{R}_{a,b} (\mathcal{L}_{a,m} \mathcal{L}_{a,m+1}) (\mathcal{L}'_{b,m} \mathcal{L}'_{b,m+1}) = (\mathcal{L}'_{b,m} \mathcal{L}'_{b,m+1}) (\mathcal{L}_{a,m} \mathcal{L}_{a,m+1}) \mathcal{R}_{a,b}, \quad (6.14b)$$

that has the form (6.13). Repeating this idea M -times, one can find the RTT-relation

$$\boxed{\mathcal{R}_{a,b}(u, v) \mathbf{T}_a(u) \mathbf{T}_b(v) = \mathbf{T}_b(v) \mathbf{T}_a(u) \mathcal{R}_{a,b}(u, v)}, \quad (6.15)$$

where $T(u)$ represents the monodromy operators

$$\begin{aligned} T_{2a}(u) &= \mathcal{L}_{2a,0}(u) \mathcal{L}_{2a,2}(u) \cdots \mathcal{L}_{2a,2M-2}(u) \\ T_{2a+1}(u) &= \mathcal{L}_{2a+1,1}(u) \mathcal{L}_{2a+1,3}(u) \cdots \mathcal{L}_{2a+1,2M-1}(u) . \end{aligned} \quad (6.16)$$

We want to close this section writing the constraints imposed by the fundamental commutation relation on the Boltzmann weights. We have seen that $\mathcal{L} \in \text{End}(\tilde{V} \otimes V \otimes V)$, where $V \simeq \tilde{V} \simeq \mathbb{C}^2$. Moreover, as we have seen before, \mathcal{L} is an 8×8 matrix, therefore, $\mathcal{R} \in \text{End}(\tilde{V} \otimes \tilde{V})$ is a 4×4 matrix, and its entries are 2×2 operators acting on the space V . Let us write

$$\mathcal{R}_{ab}|\alpha\tilde{\alpha}\rangle = \sum_{\beta\tilde{\beta}} \mathcal{R} \begin{bmatrix} \beta & \tilde{\beta} \\ \alpha & \tilde{\alpha} \end{bmatrix} |\beta\tilde{\beta}\rangle . \quad (6.17)$$

then, one can show that the Fundamental Commutation Relation gives the following constraints to the Boltzmann weights

$$\sum_{\gamma,\tilde{\gamma},\lambda_1,\lambda_2} \mathcal{R} \begin{bmatrix} u, v \begin{bmatrix} \beta & \tilde{\beta} \\ \gamma & \tilde{\gamma} \end{bmatrix} \end{bmatrix} \mathcal{W} \begin{bmatrix} u \begin{bmatrix} \nu_1 & \nu_2 \\ \alpha & \gamma \end{bmatrix} \end{bmatrix} \mathcal{W} \begin{bmatrix} v \begin{bmatrix} \lambda_1 & \lambda_2 \\ \mu_1 & \mu_2 \end{bmatrix} \end{bmatrix} = \sum_{\gamma,\tilde{\gamma},\lambda_1,\lambda_2} \mathcal{W} \begin{bmatrix} v \begin{bmatrix} \nu_1 & \nu_2 \\ \tilde{\gamma} & \tilde{\beta} \end{bmatrix} \end{bmatrix} \mathcal{W} \begin{bmatrix} u \begin{bmatrix} \lambda_1 & \lambda_2 \\ \gamma & \beta \end{bmatrix} \end{bmatrix} \mathcal{R} \begin{bmatrix} u, v \begin{bmatrix} \gamma & \tilde{\gamma} \\ \alpha & \tilde{\alpha} \end{bmatrix} \end{bmatrix} . \quad (6.18)$$

that we represent diagrammatically as in figure 16.

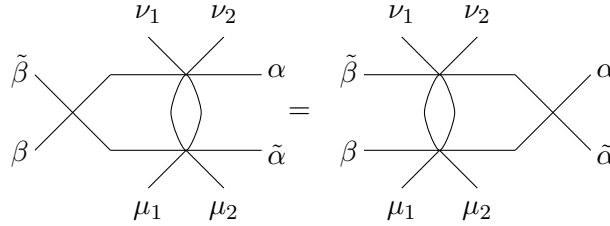


Figure 16: Diagrammatic representation of the fundamental commutation relation.

One natural question that emerges now is if we can consider these constraints on the Boltzmann weights and rebuild the Kagome lattice from these two subsystems. It is not clear if this process gives a consistent lattice.

6.3 2-particle scattering and descendant of the vertex models

The pinnacle of integrability is the factorization of an n-scattering processes into 2-scattering process, but the decomposition of the hexagons in terms of 3-particles scattering 13 seems to be a direct violation of this condition. On the other hand, we have found a the fundamental commutation relation 16 that is the underlying algebraic structure in integrable models. In this section we would like to explain this apparent conundrum.

First, remember that in each hexagon, the allowed pairs in the Y-rows are $|\circ\circ\rangle$, $|\circ\bullet\rangle$ and $|\bullet\circ\rangle$, while $|\bullet\bullet\rangle$ decouples from the system. In other words, physical states live in $\mathbb{C}^3 \subset \mathbb{C}^2 \times \mathbb{C}^2$. Observe that the X-rows states form a four dimensional space, that is $|\circ\circ\rangle_X$, $|\circ\bullet\rangle_X$, $|\bullet\circ\rangle_X$ and $|\bullet\bullet\rangle_X$ are all physical.

Consider the adjoint representation of $sl(2, \mathbb{C})$, and we denote its states as

$$|+1\rangle \equiv |\bullet\circ\rangle \quad |0\rangle \equiv |\circ\circ\rangle \quad |-1\rangle \equiv |\circ\bullet\rangle . \quad (6.19)$$

In this representation, there are 36 Boltzmann weights, but using the constraints of section 5, one can show that half of them are trivial and we recover the 18 weights in figure 12. Moreover, it is easy to rewrite the nontrivial Boltzmann weights 12 in the $sl(2, \mathbb{C})$ adjoint representation.

Now we want to rewrite (5.15) in a better form, that is

$$\mathcal{L}_{a,m}(u)|\alpha, M\rangle = \sum_{\beta M} \mathcal{W}[u | \alpha_M^N \beta] |N, \beta\rangle, \quad (6.20a)$$

where

$$|\alpha, M\rangle = |\alpha\rangle \otimes |\mu_1 \mu_2\rangle \quad |N, \beta\rangle = |\nu_1 \nu_2\rangle \otimes |\beta\rangle, \quad (6.20b)$$

and $M, N = 0, \pm 1$ with $+1 \equiv \bullet\circ$, $0 \equiv \circ\circ$ and $-1 \equiv \circ\bullet$. In other words, the Boltzmann weights are the components of $\mathcal{L}_{a,m}(u)$

$$[\mathcal{L}_{a,m}(u)]_{\alpha M}^{\beta N} \equiv \langle N, \beta | \mathcal{L}_{a,m}(u) | \alpha, M \rangle = \mathcal{W}[u | \alpha_M^N \beta]. \quad (6.20c)$$

Now, let us rewrite equations (5.16) as

$$\begin{aligned} \mathcal{L}_{a,m}|\circ\rangle|\circ\circ\rangle &= \left(\mathcal{W} \begin{bmatrix} \circ & \circ \\ \circ & \circ \end{bmatrix} |\circ\circ\rangle + \mathcal{W} \begin{bmatrix} \bullet & \circ \\ \circ & \circ \end{bmatrix} |\bullet\circ\rangle + \mathcal{W} \begin{bmatrix} \circ & \bullet \\ \circ & \circ \end{bmatrix} |\circ\bullet\rangle \right) |\circ\rangle + \left(\mathcal{W} \begin{bmatrix} \circ & \circ \\ \bullet & \circ \end{bmatrix} |\circ\circ\rangle + \mathcal{W} \begin{bmatrix} \bullet & \circ \\ \bullet & \circ \end{bmatrix} |\bullet\circ\rangle \right) |\bullet\rangle \\ \mathcal{L}_{a,m}|\circ\rangle|\bullet\circ\rangle &= \left(\mathcal{W} \begin{bmatrix} \circ & \circ \\ \bullet & \circ \end{bmatrix} |\circ\circ\rangle + \mathcal{W} \begin{bmatrix} \bullet & \circ \\ \bullet & \circ \end{bmatrix} |\bullet\circ\rangle + \mathcal{W} \begin{bmatrix} \circ & \bullet \\ \bullet & \circ \end{bmatrix} |\circ\bullet\rangle \right) |\circ\rangle + \left(\mathcal{W} \begin{bmatrix} \circ & \circ \\ \circ & \bullet \end{bmatrix} |\circ\circ\rangle + \mathcal{W} \begin{bmatrix} \bullet & \circ \\ \circ & \bullet \end{bmatrix} |\bullet\circ\rangle \right) |\bullet\rangle \\ \mathcal{L}_{a,m}|\circ\rangle|\circ\bullet\rangle &= \left(\mathcal{W} \begin{bmatrix} \circ & \circ \\ \circ & \bullet \end{bmatrix} |\circ\circ\rangle + \mathcal{W} \begin{bmatrix} \bullet & \circ \\ \circ & \bullet \end{bmatrix} |\bullet\circ\rangle + \mathcal{W} \begin{bmatrix} \circ & \bullet \\ \circ & \bullet \end{bmatrix} |\circ\bullet\rangle \right) |\circ\rangle \\ \mathcal{L}_{a,m}|\bullet\rangle|\circ\circ\rangle &= \left(\mathcal{W} \begin{bmatrix} \circ & \circ \\ \circ & \circ \end{bmatrix} |\circ\circ\rangle + \mathcal{W} \begin{bmatrix} \circ & \bullet \\ \circ & \circ \end{bmatrix} |\circ\bullet\rangle \right) |\circ\rangle + \mathcal{W} \begin{bmatrix} \circ & \circ \\ \bullet & \circ \end{bmatrix} |\circ\circ\rangle |\bullet\rangle \\ \mathcal{L}_{a,m}|\bullet\rangle|\circ\bullet\rangle &= \left(\mathcal{W} \begin{bmatrix} \circ & \circ \\ \circ & \bullet \end{bmatrix} |\circ\circ\rangle + \mathcal{W} \begin{bmatrix} \circ & \bullet \\ \circ & \bullet \end{bmatrix} |\circ\bullet\rangle \right) |\circ\rangle \end{aligned} \quad (6.21)$$

where we have kept the tensor product implicit. The Lax operator is simply

$$\mathcal{L}_{a,m} = \begin{pmatrix} \mathcal{L}_{\circ}^{\circ} & \mathcal{L}_{\circ}^{\bullet} \\ \mathcal{L}_{\bullet}^{\circ} & \mathcal{L}_{\bullet}^{\bullet} \end{pmatrix} \quad (6.22)$$

where $[\mathcal{L}_{\alpha}^{\beta}]$ are 3×3 matrices defined by

$$[\mathcal{L}_{\alpha}^{\beta}] = \begin{pmatrix} \langle \circ\circ | \mathcal{L}_{\alpha}^{\beta} | \circ\circ \rangle & \langle \circ\circ | \mathcal{L}_{\alpha}^{\beta} | \bullet\circ \rangle & \langle \circ\circ | \mathcal{L}_{\alpha}^{\beta} | \circ\bullet \rangle \\ \langle \bullet\circ | \mathcal{L}_{\alpha}^{\beta} | \circ\circ \rangle & \langle \bullet\circ | \mathcal{L}_{\alpha}^{\beta} | \bullet\circ \rangle & \langle \bullet\circ | \mathcal{L}_{\alpha}^{\beta} | \circ\bullet \rangle \\ \langle \circ\bullet | \mathcal{L}_{\alpha}^{\beta} | \circ\circ \rangle & \langle \circ\bullet | \mathcal{L}_{\alpha}^{\beta} | \bullet\circ \rangle & \langle \circ\bullet | \mathcal{L}_{\alpha}^{\beta} | \circ\bullet \rangle \end{pmatrix} \quad (6.23a)$$

with

$$\begin{aligned} \mathcal{L}_{a,m}|v\rangle \otimes |\circ\rangle &= \mathcal{L}_{\circ}^{\circ}|v\rangle \otimes |\circ\rangle + \mathcal{L}_{\circ}^{\bullet}|v\rangle \otimes |\bullet\rangle \\ \mathcal{L}_{a,m}|v\rangle \otimes |\bullet\rangle &= \mathcal{L}_{\bullet}^{\circ}|v\rangle \otimes |\circ\rangle + \mathcal{L}_{\bullet}^{\bullet}|v\rangle \otimes |\bullet\rangle. \end{aligned} \quad (6.23b)$$

Therefore

$$\begin{aligned}
\mathcal{L}_\circ^\circ | \circ \circ \rangle &= \mathcal{W} \begin{bmatrix} \circ & \circ \\ \circ & \circ \end{bmatrix} | \circ \circ \rangle + \mathcal{W} \begin{bmatrix} \bullet & \circ \\ \circ & \circ \end{bmatrix} | \bullet \circ \rangle + \mathcal{W} \begin{bmatrix} \circ & \bullet \\ \circ & \circ \end{bmatrix} | \circ \bullet \rangle \\
\mathcal{L}_\circ^\circ | \bullet \circ \rangle &= \mathcal{W} \begin{bmatrix} \circ & \circ \\ \bullet & \circ \end{bmatrix} | \circ \circ \rangle + \mathcal{W} \begin{bmatrix} \bullet & \circ \\ \bullet & \circ \end{bmatrix} | \bullet \circ \rangle + \mathcal{W} \begin{bmatrix} \circ & \bullet \\ \bullet & \circ \end{bmatrix} | \circ \bullet \rangle \\
\mathcal{L}_\circ^\circ | \circ \bullet \rangle &= \mathcal{W} \begin{bmatrix} \circ & \circ \\ \circ & \bullet \end{bmatrix} | \circ \circ \rangle + \mathcal{W} \begin{bmatrix} \bullet & \circ \\ \circ & \bullet \end{bmatrix} | \bullet \circ \rangle + \mathcal{W} \begin{bmatrix} \circ & \bullet \\ \circ & \bullet \end{bmatrix} | \circ \bullet \rangle
\end{aligned} \tag{6.24a}$$

$$\begin{aligned}
\mathcal{L}_\circ^\bullet | \circ \circ \rangle &= \mathcal{W} \begin{bmatrix} \circ & \circ \\ \circ & \bullet \end{bmatrix} | \circ \circ \rangle + \mathcal{W} \begin{bmatrix} \bullet & \circ \\ \circ & \bullet \end{bmatrix} | \bullet \circ \rangle \\
\mathcal{L}_\circ^\bullet | \bullet \circ \rangle &= \mathcal{W} \begin{bmatrix} \circ & \circ \\ \bullet & \bullet \end{bmatrix} | \circ \circ \rangle + \mathcal{W} \begin{bmatrix} \bullet & \circ \\ \bullet & \bullet \end{bmatrix} | \bullet \circ \rangle \\
\mathcal{L}_\circ^\bullet | \circ \bullet \rangle &= 0
\end{aligned} \tag{6.24b}$$

$$\begin{aligned}
\mathcal{L}_\bullet^\circ | \circ \circ \rangle &= \mathcal{W} \begin{bmatrix} \circ & \circ \\ \circ & \circ \end{bmatrix} | \circ \circ \rangle + \mathcal{W} \begin{bmatrix} \circ & \bullet \\ \circ & \circ \end{bmatrix} | \circ \bullet \rangle \\
\mathcal{L}_\bullet^\circ | \bullet \circ \rangle &= 0 \\
\mathcal{L}_\bullet^\circ | \circ \bullet \rangle &= \mathcal{W} \begin{bmatrix} \circ & \circ \\ \circ & \bullet \end{bmatrix} | \circ \circ \rangle + \mathcal{W} \begin{bmatrix} \circ & \bullet \\ \circ & \bullet \end{bmatrix} | \circ \bullet \rangle
\end{aligned} \tag{6.24c}$$

and

$$\begin{aligned}
\mathcal{L}_\bullet^\bullet | \circ \circ \rangle &= \mathcal{W} \begin{bmatrix} \circ & \circ \\ \circ & \bullet \end{bmatrix} | \circ \circ \rangle \\
\mathcal{L}_\bullet^\bullet | \bullet \circ \rangle &= 0 \\
\mathcal{L}_\bullet^\bullet | \circ \bullet \rangle &= 0
\end{aligned} \tag{6.24d}$$

Using these expressions, one can find (6.22). It is worthwhile to observe that although the physical degrees of freedom do not change, using the $sl(2, \mathbb{C})$ adjoint representation, the Lax operator is a singular 6×6 matrix, whilst in the fundamental representation we have used before, it is a 8×8 singular matrix, but we have been able to select a 5D subspace where the Lax operator \mathcal{L} has a suitable interpretation as an S-matrix.

From all these definitions, one can write the fundamental commutation relation (6.18) as

$$\boxed{\sum_{\gamma, \tilde{\gamma}, P} \mathcal{R}[u, v | \begin{smallmatrix} \beta & \tilde{\beta} \\ \gamma & \tilde{\gamma} \end{smallmatrix}] \mathcal{W}[u | \begin{smallmatrix} N \\ \alpha_P \gamma \end{smallmatrix}] \mathcal{W}[u | \begin{smallmatrix} P \\ \tilde{\alpha}_M \tilde{\gamma} \end{smallmatrix}]} = \sum_{\gamma, \tilde{\gamma}, P} \mathcal{W}[v | \begin{smallmatrix} N \\ \tilde{\gamma}_P \tilde{\beta} \end{smallmatrix}] \mathcal{W}[u | \begin{smallmatrix} P \\ \gamma_M \beta \end{smallmatrix}] \mathcal{R}[u, v | \begin{smallmatrix} \gamma & \tilde{\gamma} \\ \alpha & \tilde{\alpha} \end{smallmatrix}]] \tag{6.25}$$

Now we can represent this expression diagrammatically as figure 17, where the double line denotes the adjoint representation of $sl(2, \mathbb{C})$.

The definitions above characterized the even and odd subsystems as descendant of the vertex model [16]. More specifically, it is often assumed that the auxiliary and quantum spaces are isomorphic, but in our case, these two spaces are clearly different. As a relevant example, the 6-vertex model is defined from the fundamental representation of $su(2)$, and the Lax operator is simply $\mathcal{L}^{6v} \equiv \mathcal{L}^{(\frac{1}{2}, \frac{1}{2})} \in \text{End}(V_a \times V_q)$, where $V_a \simeq V_q \simeq \mathbb{C}^2$. Therefore

$$\mathcal{L}^{(\frac{1}{2}, \frac{1}{2})} := \begin{array}{c} V_q \\ | \\ V_a \text{ --- } V_a \\ | \\ V_q \end{array} \tag{6.26}$$

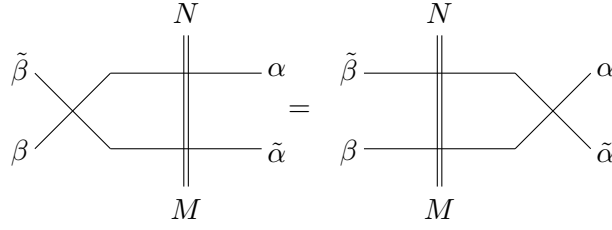


Figure 17: Diagrammatic representation of the fundamental commutation relation.

The subsystem defined in this section, which culminated in the fundamental commutation relation 17 is defined by a Lax operator of the form $\mathcal{L} \equiv \mathcal{L}^{(\frac{1}{2},1)} \in \text{End}(V_a \times \tilde{V}_q)$, where $\tilde{V}_q \simeq \mathbb{C}^3$, so that

$$\mathcal{L}^{(\frac{1}{2},1)} := \begin{array}{c} \tilde{V}_q \\ \parallel \\ V_a \text{ --- } \parallel \text{ --- } V_a \\ \parallel \\ \tilde{V}_q \end{array} \quad (6.27)$$

where the double line denotes the adjoint representation of $sl(2, \mathbb{C})$. A clear exposition of these descendant models, including the Bethe ansatz analysis, can be found in section §2.4 of [16].

7 Conclusions and Perspectives

In this paper we continue our analysis of the Kagome lattice system introduced in [13]. The most appealing aspect of this system is its Hilbert space with a plane partitions grading. We expect that these new aspects shed some light on the quantum crystal melting integrability.

In section 2, we write the Kagome lattice system as a stack of two types of spin chains, that we called X - and Y -rows, which are respectively defined in terms of two fermionic fields with components ψ_m and $\theta_{m+1/2}$, with $m \in \mathbb{Z}$. This description brings the discussion to a formalism closer to the one considered in [11]. Physical states, which are classified by plane partitions, were considered in section 3. We have found explicit expressions for the plane partitions growth operators, and for states corresponding to the 0-, 1- and 2-boxes partitions.

Moreover, it is an important exercise to compare the results of this section with the 2D case in [11], where all integer partitions can be easily written once the growth operators and a reference state defined by the filled Fermi sea are properly considered. In the present case, we need to define two families of reference states (since we have two types of rows, the X and Y -chains), and these reference states are generally harder than the filled Fermi sea. Quite remarkably, these reference states are manageable, as we show in section 3, and the construction of plane partitions states is almost immediate once the 0-box configuration is properly defined.

Furthermore, in section 4 we also write the crystal melting Hamiltonian using the formalism we develop in section 2. Contrary to the 2D case [11], it is not immediately clear if the 3D problem is exactly solvable.

In section 5, we consider an associate classical statistical system that is defined when we

assign Boltzmann weights for the allowed hexagon configurations. In other words, we have shown that the plane partition growth can be completely defined with 18 different local configurations, and if we assign a Boltzmann weight to each of these, we find a statistical problem that is not very different from the vertex models. In section 6, we show that one can study the classical system using two types of row-to-row transfer matrices, say \mathbf{t} and $\tilde{\mathbf{t}}$, but since $[\mathbf{t}(u), \tilde{\mathbf{t}}(v)] \neq 0$, we cannot build commuting conserved charges from these objects. We should remark, though, that this result does not disprove the integrability of the classical model, it simply says that the integrability, if present, cannot be addressed by \mathbf{t} and $\tilde{\mathbf{t}}$.

Section 6 also concludes this paper with a curious analysis. Notwithstanding the noncommutativity $[\mathbf{t}(u), \tilde{\mathbf{t}}(v)] \neq 0$, the transfer matrices \mathbf{t} and $\tilde{\mathbf{t}}$ do commute among themselves, that is $[\mathbf{t}(u), \mathbf{t}(v)] = 0$ and $[\tilde{\mathbf{t}}(u), \tilde{\mathbf{t}}(v)] = 0$, and can be used to define two completely equivalent integrable subsystems. These models descend from the 6 vertex model, and it is assumed that the states in the X -spin chains fulfill a fundamental representation of the $su(2)$ while the pair of states in the Y -spin chains are associated to the $sl(2, \mathbb{C})$ adjoint representation. We hope to address further aspects of this observation in a future publication.

There are many possible directions of research, here is a short (and biased) list of interesting problems. The system we defined in section 5 seems to be a rich statistical model, and given the results we found, the most immediate question is to what extent the Yang-Baxter subsystems, the descendant of the 6-vertex model, can be used as building blocks for plane partitions. In other words, given any solution to the descendant vertex models, can we use its Boltzmann weights to address the crystal melting problem? In fact, the classical statistical system above has a much bigger physical space, so it is important to develop techniques to separate the macroscopic states with corresponding plane partitions analogues from those states without such a description.

In this paper, and in [13], we have studied just one of the two conjectures of [11], namely, the one related to the integrability of the 3D problem. We have not touched, yet, the second (and perhaps more interesting) conjecture on the mass gap of this system. One natural question is if the ideas we developed here and in [13] can help to prove or disprove the mass gap conjecture of [11].

Finally, we should also point that the original motivation for the crystal melting problem was to shed some light on a variety of relations between plane partitions and $N = 2$ supersymmetric theories, topological strings, the AGT and the AdS3/Higher spin correspondence [9, 14, 15]; and we have not addressed any of these connections yet. This particular problem is currently under investigation and we hope to provide some answers in a future publication. Let us hope nature does not disappoint us.

Acknowledgements I am supported by the Swiss National Science Foundation under grant number PP00P2_183718/1. I would also like to thank Susanne Reffert and Domenico Orlando for many discussions and collaborations on related projects.

References

- [1] M. Niss, “History of the LenzIsing Model 19501965: from irrelevance to relevance,” *Archive for History of Exact Sciences* **63** (2008) 243.
<https://doi.org/10.1007/s00407-008-0039-5>.

- [2] N. Hitchin, R. Nigel J. Hitchin, N. Hitchin, S. Hitchin, G. Segal, N. Woodhouse, R. Ward, L. Segal, O. Conference on Integrable Systems (1997, O. Conference on Integrable Systems. 1997, *et al.*, *Integrable Systems: Twistors, Loop Groups, and Riemann Surfaces*. Oxford Graduate Texts in Mathematics. Clarendon Press, 1999.
<https://books.google.ch/books?id=SSwSDAAAQBAJ>.
- [3] T. Miwa, M. Jinbo, M. Jimbo, E. Date, M. Reid, W. Fulton, A. Katok, F. Kirwan, B. Bollobas, P. Sarnak, *et al.*, *Solitons: Differential Equations, Symmetries and Infinite Dimensional Algebras*. Cambridge Tracts in Mathematics. Cambridge University Press, 2000.
<https://books.google.ch/books?id=kQDw1ZcqLjUC>.
- [4] P. MacMahon, *Combinatory Analysis*. No. v. 1 in Combinatory Analysis. The University Press, 1915. <https://books.google.ch/books?id=qvLuAAAAMAAJ>.
P. MacMahon, *Combinatory Analysis*. No. v. 2 in Combinatory Analysis. The University Press, 1916. https://books.google.ch/books?id=A_PuAAAAMAAJ.
- [5] A. Okounkov, N. Reshetikhin, and C. Vafa, “Quantum Calabi-Yau and classical crystals,” *Prog. Math.* **244** (2006) 597, [arXiv:hep-th/0309208](https://arxiv.org/abs/hep-th/0309208) [hep-th].
- [6] N. Nekrasov and A. Okounkov, “Seiberg-Witten theory and random partitions,” [arXiv:hep-th/0306238](https://arxiv.org/abs/hep-th/0306238).
- [7] J. J. Heckman and C. Vafa, “Crystal Melting and Black Holes,” *JHEP* **09** (2007) 011, [arXiv:hep-th/0610005](https://arxiv.org/abs/hep-th/0610005).
- [8] A. Okounkov, “The uses of random partitions,” [arXiv:math-ph/0309015](https://arxiv.org/abs/math-ph/0309015) [math-ph].
- [9] M. R. Gaberdiel, R. Gopakumar, W. Li, and C. Peng, “Higher Spins and Yangian Symmetries,” *JHEP* **04** (2017) 152, [arXiv:1702.05100](https://arxiv.org/abs/1702.05100) [hep-th].
- [10] R. Kenyon, “An introduction to the dimer model,” [arXiv:math/0310326](https://arxiv.org/abs/math/0310326) [math.CO].
- [11] R. Dijkgraaf, D. Orlando, and S. Reffert, “Quantum Crystals and Spin Chains,” *Nucl. Phys. B* **811** (2009) 463–490, [arXiv:0803.1927](https://arxiv.org/abs/0803.1927) [cond-mat.stat-mech].
- [12] D. Orlando, S. Reffert, and N. Reshetikhin, “On domain wall boundary conditions for the XXZ spin Hamiltonian,” [arXiv:0912.0348](https://arxiv.org/abs/0912.0348) [math-ph].
- [13] T. Araujo, D. Orlando, and S. Reffert, “Quantum crystals, Kagome lattice and plane partitions fermion-boson duality,” [arXiv:2005.09103](https://arxiv.org/abs/2005.09103) [hep-th].
- [14] D. Maulik and A. Okounkov, *Quantum Groups and Quantum Cohomology*. Société Mathématique de France, 2019. [arXiv:1211.1287](https://arxiv.org/abs/1211.1287) [math.AG].
<https://books.google.ch/books?id=9lTUxQEACAAJ>.
- [15] T. Prochazka, “ \mathcal{W} -symmetry, topological vertex and affine Yangian,” *JHEP* **10** (2016) 077, [arXiv:1512.07178](https://arxiv.org/abs/1512.07178) [hep-th].
- [16] C. Gomez, G. Sierra, and M. Ruiz-Altaba, *Quantum groups in two-dimensional physics*. Cambridge Monographs on Mathematical Physics. Cambridge University Press, 2011.